Recent progress on superconductors with time-reversal symmetry breaking

Sudeep Kumar Ghosh,[1,*] Michael Smidman,[2,3,†] Tian Shang,[4,5] James F. Annett,[6] Adrian Hillier,[7] Jorge Quintanilla,[1] and Huiqiu Yuan[2,3,8,9,‡]

[1] *Physics of Quantum Materials, School of Physical Sciences, University of Kent, Canterbury CT2 7NH, United Kingdom*
[2] *Center for Correlated Matter and Department of Physics, Zhejiang University, Hangzhou 310058, China*
[3] *Zhejiang Province Key Laboratory of Quantum Technology and Device, Department of Physics, Zhejiang University, Hangzhou 310027, China*
[4] *Laboratory for Multiscale Materials Experiments, Paul Scherrer Institut, Villigen CH-5232, Switzerland*
[5] *Physik-Institut, Universitt Zürich, Winterthurerstrasse 190, CH-8057 Zürich, Switzerland*
[6] *H. H. Wills Physics Laboratory, University of Bristol, Tyndall Avenue, Bristol BS8 1TL, United Kingdom*
[7] *ISIS Facility, STFC Rutherford Appleton Laboratory, Harwell Science and Innovation Campus, Didcot OX11 0QX, United Kingdom*
[8] *State Key Laboratory of Silicon Materials, Zhejiang University, Hangzhou 310027, China*
[9] *Collaborative Innovation Center of Advanced Microstructures, Nanjing University, Nanjing 210093, China*

(Dated: July 21, 2020)

Superconductivity and magnetism are adversarial states of matter. The presence of spontaneous magnetic fields inside the superconducting state is, therefore, an intriguing phenomenon prompting extensive experimental and theoretical research. In this review, we discuss recent experimental discoveries of unconventional superconductors which spontaneously break time-reversal symmetry and theoretical efforts in understanding their properties. We discuss the main experimental probes and give an extensive account of theoretical approaches to understand the order parameter symmetries and the corresponding pairing mechanisms, including the importance of multiple bands.

I. INTRODUCTION

Spontaneously broken symmetry is a cornerstone of our current understanding of the physical world[1]. The superconducting state is one of the most spectacular examples: by spontaneously breaking global gauge symmetry, a superconductor's wave function becomes macroscopically coherent - electrons in a superconductor (SC) behave analogously to photons in a laser. This review is concerned with unconventional SCs where an additional symmetry is broken in the superconducting state, namely time-reversal symmetry (TRS).

In classical physics, time reversal is equivalent to reversing the momenta of all the particles in the system. Time-reversal symmetry refers to the fact that when this is done, the trajectories we obtain are also valid solutions of the equations of motion. Because of this, any thermal average characterizing the macroscopic state of an ergodic system with TRS must be invariant under time-reversal. Since time-reversal flips the sign of angular momenta, and therefore of the magnetic moments, it follows that an ergodic system with TRS cannot have a net magnetization. The same consideration applies to quantum many-body systems though in this case the spin of the particles constitutes an additional contribution to the angular momentum and therefore time-reversal involves the reversal of all spins in addition to the change of sign of all momenta[2]. Mathematically, this is ensured by the following transformation

$$\mathcal{T} c^{\dagger}_{\boldsymbol{k}\uparrow} = -c_{-\boldsymbol{k}\downarrow} \;\; ; \;\; \mathcal{T} c^{\dagger}_{\boldsymbol{k}\downarrow} = c_{-\boldsymbol{k}\uparrow} \tag{1}$$

where $c^{\dagger}_{\boldsymbol{k}\sigma}$ is an operator creating an electron with spin $\sigma \in \{\uparrow, \downarrow\}$ and crystal momentum $\boldsymbol{k}$ and $\mathcal{T}$ is the TRS operator.

TRS can be broken through the application of external fields or spontaneously. The canonical example of the former in solid-state physics is the electron fluid in a metal in the presence of a magnetic field, leading to Pauli paramagnetism, Landau diamagnetism and the de Haas-van Alphen effect[3]. The most obvious example of the latter is a Stoner ferromagnet, where a self-consistent exchange field leads to a net magnetization. TRS has important consequences in theories of cosmology as well. For example, in the physics of blackholes, the loop quantum gravity theory predicts that the interior of a blackhole must continue into a white hole[4,5]. This transition of a blackhole to a whitehole is analogous to a bouncing ball in classical physics: a blackhole "bounces" and emerges as its time-reversed version, a whitehole.

The superconducting state is a condensate of pairs of electrons, called "Cooper pairs". It is characterized by a complex order parameter which is usually a scalar function with an amplitude and a phase characterizing macroscopic quantum coherence. In all SCs, $U(1)$ gauge symmetry is spontaneously broken at the superconducting transition, and it is this gauge-symmetry breaking which leads to phenomena such as the Meissner and Josephson effects. In so-called "conventional" SCs, additional symmetries are not broken in the superconducting state, and the properties are well described by Bardeen-Cooper-Schrieffer (BCS) theory[6]. On the other hand, in many so-called "unconventional" SCs additional symmetries, such

as the space-group symmetries of the crystalline lattice are broken. One example is the breaking of the C_4 lattice symmetry by the $d_{x^2-y^2}$ state in the cuprates. This review is concerned with SCs that break time-reversal symmetry, which leads to the appearance of spontaneous magnetic fields in the superconducting state– a particularly dramatic manifestation of unconventional pairing as all known SCs exhibit perfect diamagnetism *via* the Meissner effect, supporting a long-held view that magnetism and superconductivity are antagonistic states of matter.

Evidence for TRS breaking was initially detected in a few highly correlated SCs using the muon-spin relaxation (μSR) technique. μSR has proved ideal for searching for broken TRS in superconducting systems, since it is a local probe capable of detecting very small magnetic fields in a sample, in the absence of an applied magnetic field. For a number of reasons, superconductivity with broken TRS has become a topic of particular interest recently. One reason is the discovery of SCs with weak-electronic correlations, where signatures of TRS breaking are detected using μSR, but other superconducting properties appear to largely resemble those of conventional systems. These therefore appear to correspond to a class of materials distinct from the previously known examples of TRS breaking SCs, and determining the origin of the broken TRS requires further experimental and theoretical attention. Furthermore, even amongst the established examples, various outstanding questions remain. In particular, Sr_2RuO_4 had long been regarded as the canonical example of a triplet SC, with a chiral p-wave order parameter[7]. This understanding has been thrown into question however, by recent nuclear magnetic resonance (NMR) measurements which point to singlet-pairing[8]. This has stimulated a flurry of experimental and theoretical studies aimed at understanding the results. Moreover, in the last decade there has been a growing appreciation of the role-played by topology in determining the properties of condensed matter systems, and topological superconductivity is one of the most sought after goals in this field. As such there has been particular interest in whether unconventional TRS breaking superconducting states can exhibit this phenomenon.

In this review, we will be mostly concerned with systems where the TRS is likely broken by the superconducting phase (this excludes systems where another phase transition is responsible for the breaking of TRS, including ferromagnetic SCs[9]). Barring fine-tuning, the breaking of TRS at the superconducting critical temperature requires a degenerate instability channel leading to a multi-component order parameter. This is because under the application of the time-reversal operator, the order parameter transforms into another order parameter which is not just a phase multiple of the original one. This is satisfied by an order parameter having multiple components and a nontrivial phase difference between them. The degeneracy of the corresponding instability channel can have many different origins. For example, it can arise from breaking underlying symmetries of the crystal, as in the chiral p-wave state[7] or the loop-super current state proposed for multi-orbital systems[10]; or it can arise from breaking the group of spin rotations, as in the nonunitary triplet state with equal spin pairing proposed for $LaNiC_2$ and $LaNiGa_2$[11–15].

A desired milestone in the study of unconventional superconductivity is to uniquely determine the structure of the order parameter and the corresponding pairing mechanism. Approaching this goal for a specific material needs experimental and theoretical knowledge to work in unison. By considering the experimentally observed properties of a system, the possible symmetry-allowed order parameters can be determined. These possibilities are then considered in mean-field theories with a model band structure or full first-principles band structure to predict low-energy properties of the material which are compared with the corresponding experimental data. A crucial means of determining the nature of the pairing state, is the characterization of the magnitude and structure of the superconducting energy gap. This can be probed using a number of techniques, including the measurement of thermodynamic quantities such as the specific heat and magnetic penetration depth, spectroscopic techniques such as angle-resolved photoemission spectroscopy (ARPES) and scanning tunneling spectroscopy, or experiments utilizing Josephson tunneling. The structure and shape of the normal state Fermi surfaces computed from first principles or measured by de Haas-van Alphen and ARPES experiments[16] can also help in narrowing-down the possible order parameter structures. However, very often, mainly due to the high symmetry of the crystal structure of the material in question, the above procedure leads to many different possible order parameters with similar low-energy properties. Thus in practice the unequivocal determination of the structure of the order parameter of a TRS-breaking SC is often very challenging.

This review article is broadly divided into two parts: 1) Experimentally discovered TRS breaking SCs with discussion of the corresponding experimental techniques and 2) Theoretical understanding of the possible structures of order parameters and low-energy properties of such materials. In Section II we briefly discuss the main experimental probes used to directly measure and characterize TRS breaking in SCs. Section III describes systems where TRS breaking has been discovered in the superconducting state, including examples in strongly correlated SCs as well as the more recent cases in materials which usually exhibit fully-open gaps. A summary of TRS breaking SCs is also provided in Table I. We then go on in Section IV to discuss the possible structures of order parameters of SCs based on general symmetry arguments within the Ginzburg-Landau theory, that is without requiring the details of the pairing mechanism and hence should apply to most unconventional SCs. In the next Section V, we focus on the order parameter symmetries of TRS breaking SCs considering some spe-

cific examples. In the Section VI we discuss the method for computing the properties of superconducting ground states within the mean-field approximation, which in its full form requires using a specific model of the pairing interaction and the normal state band-structure. In the following Section VII we discuss recent theoretical proposals of novel superconducting ground states for specific, recently-discovered TRS-breaking superconducting materials. Finally in Section VIII we conclude by outlining some possible future directions.

II. EXPERIMENTAL PROBES

Here, we briefly review the three main experimental probes which can *directly* detect the presence of spontaneous magnetic fields in the superconducting state, so as to detect TRS breaking in SCs: μSR, the optical Kerr effect and superconducting quantum interference device (SQUID) magnetometry.

A. Muon spin relaxation

μSR is a very sensitive local probe of extremely small magnetic fields in a sample (down to $\sim 10^{-5}$T). As a result, μSR measurements performed in the absence of an external field can reveal the spontaneous appearance of very small magnetic fields in the superconducting state, and hence whether TRS is broken. A particular advantage of this technique is that the presence of TRS breaking can be probed in both single crystal and polycrystalline samples. More comprehensive descriptions of the μSR technique can be found in Refs. 17–20 but here we discuss a few pertinent aspects.

Spin polarized positive muons are implanted in the sample, which stop at interstitial positions in the crystal lattice corresponding to minima of the Coulomb potential. Muons decay with a half life of 2.2μs into a positron and two neutrinos, and the emitted positrons are counted via detectors which in the experiments described here are situated in forward (F) and backward (B) positions. The muons' spins precess about the local magnetic fields at the muon stopping sites $\mathbf{B}_{\rm loc}$, at the Larmor frequency $\omega_\mu = \gamma_\mu |\mathbf{B}_{\rm loc}|$, where $\gamma_\mu/2\pi = 135.5$ MHz T^{-1} is the muon gyromagnetic ratio. Since the positrons are emitted preferentially along the direction of the muon spin, the asymmetry $A(t)$ reflects the local field distribution, where

$$A(t) = \frac{N_F(t) - \alpha N_B(t)}{N_F(t) + \alpha N_B(t)}. \tag{2}$$

Here $N_F(t)$ and $N_B(t)$ are the number of positrons counted at a time t at the forward and backward detectors respectively, while α is a calibration constant. In particular, when there is a distribution of fields in a sample, the muons' spins precess at different rates, and the broader the field distribution, the more rapidly $A(t)$ decays. Time reversal symmetry breaking is experimentally detected from an increase of the relaxation rate of $A(t)$, arising due to the spontaneous appearance of additional internal fields in the superconducting state. For a random static Gaussian distribution of fields, $A(t)$ is described by the Kubo-Toyabe relaxation function

$$G_{KT} = \frac{1}{3} + \frac{2}{3}(1 - \sigma_{\rm ZF}^2 t^2) e^{-\frac{\sigma_{\rm ZF}^2 t^2}{2}}, \tag{3}$$

where the Gaussian relaxation rate $\sigma_{\rm ZF}$ is proportional to the width of the field distribution. Since nuclear moments are static on the timescale of the muon lifetime, these make a temperature independent contribution to $\sigma_{\rm ZF}$. In most of the cases discussed here, the asymmetry was fitted with the product of G_{KT} with a Lorentzian relaxation

$$A(t) = A_0 G_{KT}(t) e^{-\lambda_{\rm ZF} t}, \tag{4}$$

where A_0 is the initial asymmetry and $\lambda_{\rm ZF}$ is the Lorentzian relaxation rate. On the other hand, sometimes a combined Lorentzian and Gaussian Kubo-Toyabe function is utilized,

$$A(t) = A_0 \frac{1}{3} + \frac{2}{3}(1 - \sigma_{\rm ZF}^2 t^2 - \lambda_{\rm ZF} t) e^{-\frac{\sigma_{\rm ZF}^2 t^2}{2} - \lambda_{\rm ZF} t}. \tag{5}$$

In some experiments, the TRS breaking is manifested by an increase of $\sigma_{\rm ZF}$ in the superconducting state, in others it is via $\lambda_{\rm ZF}$. Note that $\lambda_{\rm ZF}$ is often attributed to magnetic fields which fluctuate rapidly on the timescale of the muon lifetime, i.e. 'electronic' moments, since such a Lorentzian decay results from a Gaussian distribution of fields in the fast fluctuation limit. However in TRS breaking SCs, the increase in $\lambda_{\rm ZF}$ or $\sigma_{\rm ZF}$ is typically suppressed by a small longitudinal field of around 20 mT. The fact that the muon can be decoupled from its local environment by a small longitudinal field indicates that these internal fields are quasistatic. This suggests that this extra relaxation does not arise from paramagnetic impurities. As displayed in Table I, the increased relaxation rate below T_c in SCs with broken TRS corresponds to spontaneous magnetic fields smaller than 0.1 mT.

B. Optical Kerr effect

The optical Kerr effect is another very sensitive probe for detecting spontaneous fields inside a SC by measuring the change in the Kerr angle. Due to the technically challenging nature of these experiments, TRS breaking has been observed using the Kerr effect in only a few SCs. Moreover, the reliable determination of the presence of broken TRS generally requires single crystal, rather than polycrystalline samples. The quantity measured in

these experiments is the polar Kerr angle θ_K, which corresponds to how much normally incident linearly polarized light is rotated[21–25]. Non-zero θ_K arises from differences between the complex refractive indices of left (n_L) and right (n_R) circularly polarized light via

$$\theta_K = -\mathrm{Im}\left(\frac{n_R - n_L}{n_L n_R - 1}\right) = \mathrm{Im}\frac{4\pi}{\omega}\left(\frac{1}{n(n^2-1)}\sigma_{xy}\right). \quad (6)$$

As such, θ_K is related to the presence of an imaginary component to the off-diagonal part of the conductivity tensor σ_{xy}, which only arises when time reversal symmetry is broken. In SCs this requires that the superconducting order parameter has multiple components with a phase between them[24]. In order to detect the TRS breaking signal, it is necessary to measure a very small θ_K on the order of 1 μrad, yet with a sufficiently low beam intensity to avoid sample heating. These were performed using a Sagnac interferometer, as described in detail in Refs. 21, 22, 26, and 27 where the authors achieve a sensitivity in θ_K of 10 nrad, at temperatures down to 100 mK. Due to the presence of different domains, upon zero-field cooling (ZFC) there may be no net contribution to θ_K. Therefore, in addition to measuring θ_K after cooling in zero-field, a training field was often applied in the superconducting state to align the domains. The field was then turned off, and measurements were performed upon warming to above T_c. Upon reversing the direction of the training field, θ_K has the same magnitude but opposite sign below T_c, and therefore the magnetic field couples to and reorientates the domains. In the cases of Sr_2RuO_4, UPt_3 and URu_2Si_2[21–23], the magnitude of θ_K after applying the training field is the same as in the ZFC measurements, indicating that the domain size is larger than the diameter of the beam (≈ 10.6 μm).

C. SQUID magnetometry

SQUID magnetometry can in principle be used to detect broken TRS, if the system develops a small net magnetization as it enters the superconducting state. Though the field resulting from such a magnetization will be fully screened by the Meissner effect in the bulk of the sample, in a type-II SC the superconducting order parameter will be suppressed near the surface, allowing the magnetic field due to the bulk magnetization to be detected. One major problem with this approach is that even large domains will be averaged out, since one is measuring the signal from the whole sample. Nevertheless as we discuss below this technique has been successfully employed to detect a net magnetization in $LaNiC_2$[34].

III. SUPERCONDUCTORS WITH BROKEN TIME REVERSAL SYMMETRY

A. TRS breaking in strongly correlated superconductors

The first reported examples of TRS breaking were in a handful of strongly correlated SCs, the properties of which are included in Table I. In such systems, the presence or close proximity of magnetism, together with the large Coulomb repulsion already gave a strong indication that the superconductivity must be unconventional, and is likely mediated by magnetic interactions. UBe_{13} was one of the earliest heavy fermion SCs to be discovered, where it was proposed to be an example of triplet p-wave pairing[35]. For heavy fermion SCs, the extremely large onsite Coulomb repulsion has been thought to disfavor s-wave superconductivity, and instead pairing states with non-zero orbital angular momentum have generally been anticipated. Unusual behavior was quickly found upon doping with Th in the $U_{1-x}Th_xBe_{13}$ system, where a second superconducting transition in the specific heat emerges at around $x = 0.03$, and disappears at $x = 0.06$[36]. Zero-field μSR subsequently revealed that while no change of σ_{ZF} is found in the superconducting state of stoichiometric UBe_{13}, an increase is observed at the second transition induced by Th-doping, as displayed in Fig. 1(a)[32]. One of the scenarios proposed was that this corresponds to a transition into a state with a complex multicomponent order parameter, which breaks TRS[37].

Perhaps the two canonical examples of SCs with strong electronic correlations exhibiting TRS breaking, although neither without controversy, are Sr_2RuO_4[7,21,33] and UPt_3[22,38]. UPt_3 is another notable early example of a heavy fermion SC, where two transitions in the zero-field specific heat are observed in stoichiometric samples, clearly indicating an unconventional superconducting order parameter[39] (for a detailed review see Ref. 40). Zero-field μSR measurements of UPt_3 by Luke *et al.* revealed a clear increase of the Lorentzian relaxation rate in the superconducting state below the lower critical temperature[38]. Here the stoichiometric nature of the system compared to the aforementioned $U_{1-x}Th_xBe_{13}$ allowed the authors to exclude the scenario of an impurity induced magnetic transition, giving a strong indication of TRS breaking. This result was corroborated much more recently by measurements of the optical Kerr rotation[22]. Evidence was also found for TRS breaking in URu_2Si_2, as displayed in Fig. 1(b), and very recently, UTe_2 using the same technique[23,41]. In the case of the UTe_2, μSR measurements exhibited a strong temperature dependent relaxation corresponding to ferromagnetic fluctuations, and therefore whether TRS is preserved in the superconducting state could not be probed[42]. For Kerr rotation measurements of UPt_3, the onset of TRS breaking could be shown to occur at the lower superconducting transition. This is expected for the proposal of triplet su-

TABLE I. Properties of TRS breaking superconductors. S and N in the space group column denote symmorphic and non-symmorphic crystal structures respectively, while CS denotes whether the crystal structure is centrosymmetric and the column headed TRSB evidence displays the techniques from which TRS breaking was deduced. The internal field $B_{\rm int}$ was calculated from the increase of the μSR relaxation rate below T_c, i.e. $B_{\rm int} = \sqrt{2}\Delta\sigma_{\rm ZF}/\gamma_\mu$ or $B_{\rm int} = \Delta\lambda_{\rm ZF}/\gamma_\mu$, when the signature for TRS breaking occurs in the Gaussian or Lorentzian channels, respectively. References not provided in the main text, are also displayed.

Compound	TRSB evidence	$B_{\rm int}$ (mT)	Structure	Space group	Point group	CS?	Gap structure	Proposed state
$U_{1-x}Th_xBe_{13}$	μSR	0.07	Cubic	$Fm\bar{3}c$ (S)	O_h	✓	–	–
UPt_3	μSR, Kerr	0.01	Hexagonal	$P6_3/mmc$ (N)	D_{6h}	✓	line node	E_{2u} triplet
URu_2Si_2	Kerr		Tetragonal	$I4/mmm$ (S)	D_{4h}	✓	line + point nodes	chiral d-wave
UTe_2[28,29]	Kerr		Orthorhombic	$Immm$ (S)	D_{2h}	✓	point nodes	non-unitary/ chiral triplet
Sr_2RuO_4	μSR, Kerr	0.05	Tetragonal	$I4/mmm$ (S)	D_{4h}	✓	line node	chiral singlet
$Ba_{1-x}K_xFe_2As_2$ ($0.7 \lesssim x \lesssim 0.85$)	μSR	0.01	Tetragonal	$I4/mmm$ (S)	D_{4h}	✓		$s+is$
$Pr(Os_{1-x}Ru_x)_4Sb_{12}$	μSR, Kerr	0.06	Cubic	$Im\bar{3}$ (S)	T_h	✓	full gap, point node	multicomponent d-wave
$Pr_{1-y}La_yOs_4Sb_{12}(y<1)$	μSR	0.06	Cubic	$Im\bar{3}$ (S)	T_h	✓	full gap, point node	–
$Pr_{1-y}La_yPt_4Ge_{12}(y<1)$	μSR	0.02	Cubic	$Im\bar{3}$ (S)	T_h	✓	point node	non-unitary p-wave
SrPtAs	μSR	0.007	Hexagonal	$P6_3/mmc$ (N)	D_{6h}	✓	full gap	chiral d-wave
CaPtAs	μSR	0.08	Tetragonal	$I4_1md$ (N)	C_{4v}	×	nodal multigap	
$Re_{0.82}Nb_{0.18}$	μSR	0.04	Cubic	$I\bar{4}3m$ (S)	T_d	×	full gap	LSC
Re_6(Zr,Hf,Ti)	μSR	0.02	Cubic	$I\bar{4}3m$ (S)	T_d	×	full gap	LSC
Re	μSR	0.02	Hexagonal	$P6_3/mmc$ (N)	D_{6h}	✓	full gap	–
$LaNiC_2$	μSR, SQUID	0.01	Orthorhombic	$Amm2$ (S)	C_{2v}	×	two full gaps	INT
$LaNiGa_2$	μSR	0.02	Orthorhombic	$Cmmm$ (S)	D_{2h}	✓	two full gaps	INT
La_7(Ir,Rh)$_3$	μSR	0.01	Hexagonal	$P6_3mc$ (N)	C_{6v}	×	full gap	singlet dominated mixed state
Zr_3Ir[30,31]	μSR	0.008	Tetragonal	$I\bar{4}2m$ (S)	D_{2d}	×	full gap	singlet dominated mixed state
(Lu,Y,Sc)$_5Rh_6Sn_{18}$	μSR	0.06	Tetragonal	$I4_1/acd$ (N)	D_{4h}	✓	full gap	multicomponent singlet or triplet

perconductivity with an E_{2u} order parameter[40,43], where the order parameter picks up a second component at the lower transition, giving rise to a complex superposition. One curious aspect is that a subsequent zero-field μSR study failed to detect an increase of the μSR relaxation rate within the superconducting state of UPt_3[44]. The authors of the later study explain this discrepancy as being due to a higher sample quality, attributing the previous findings to the presence of defects or impurities.

Sr_2RuO_4 has been one of the most extensively characterized unconventional superconducting systems, owing in a large part to the system having the same structure as

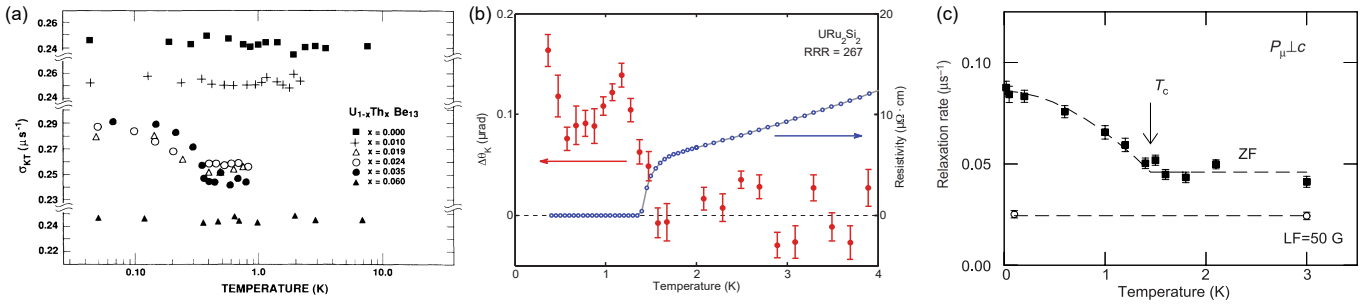

FIG. 1. (a) Temperature dependence of the Gaussian relaxation rate obtained from zero-field μSR measurements of $U_{1-x}Th_xBe_{13}$ for different dopings. For stoichiometric UBe_{13}, no change is observed below T_c, but for 2-4% Th-doping, an increase in the relaxation rate is observed below the emergent second superconducting transition. Reproduced with permission from Ref. 32. Copyright 1990 by the American Physical Society. (b) Temperature dependence of the Kerr angle and resistivity of URu_2Si_2. The increase of the Kerr angle indicates the breaking of time reversal symmetry, and it can be seen that this onsets at the superconducting transition. Reproduced with permission from Ref. 23. Copyright 2015 by the American Physical Society. (c) Temperature dependence of the Lorentzian relaxation rate (λ_{ZF} in Eq. 4) obtained from zero-field μSR on Sr_2RuO_4, with the initial muon spin polarized perpendicular to the c-axis. This quantity shows an increase below T_c indicating TRS breaking, while this effect is destroyed by a longitudinal field of 50 mT. Reproduced with permission from Macmillan Publishers Ltd: Nature[33], copyright 1998.

the high-T_c cuprates, but it was long thought to be a rare example of spin-triplet superconductivity outside of the U-based heavy fermion SCs (see Ref. 7 for a review). Evidence for TRS breaking was reported from zero-field μSR measurements on single crystals of Sr_2RuO_4, as displayed in Fig. 1(c)[33]. An increase of the Lorentzian relaxation rate λ_{ZF} is observed when the muon spin is polarized both parallel and perpendicular to the c-axis. Although λ_{ZF} in μSR measurements is often associated with rapidly fluctuating fields, the fact that the effect is destroyed by a longitudinal field of 50 mT was taken as evidence that these fields are static on the timescale of the muon lifetime, and they were estimated to have a characteristic strength of 0.5 G.

The primary evidence for spin-triplet superconductivity came from ^{17}O NMR measurements, which suggested that the Knight shift, and hence the spin-susceptibility, remains unchanged along all directions upon cooling through the superconducting transition at $T_c \approx 1.5$ K[57]. This conclusion was also supported by polarized neutron scattering measurements of the spin susceptibility[58]. The combination of TRS breaking and triplet superconductivity naturally led to the proposal of a chiral p-wave $p_x + ip_y$ pairing[7]. However, there continued to be a number of outstanding issues, namely that the Knight shift appeared to be constant along all field directions[57], suggesting that the triplet order parameter $\mathbf{d}(\mathbf{k})$ rotates with the applied field, but the spin-orbit coupling would be expected to be sufficiently strong to pin $\mathbf{d}(\mathbf{k})$ along a particular crystallographic axis. Moreover, T_c did not show the expected cusp in strain experiments[59], and both scanning SQUID and scanning Hall probe microscopy measurements did not find evidence for the currents anticipated to emerge at domain edges[60,61].

The long held understanding of chiral p-wave superconductivity[62] in Sr_2RuO_4 has been challenged by the recent findings of a decrease in the Knight shift below T_c in ^{17}O NMR measurements for in-plane fields[8], which is contrary to both earlier NMR studies[57], as well as the expected temperature-independent behavior for chiral p-wave pairing. While triplet states with $\mathbf{d}(\mathbf{k}) \perp c$ could not be completely excluded, these are not expected to exhibit TRS breaking. Moreover, this surprising result has been corroborated by subsequent spin-susceptibility measurements using polarized neutron scattering, where a drop of around 34% was detected at low temperatures compared to the value above T_c[63]. Spin-singlet superconductivity which preserves TRS was proposed from mapping the momentum dependence of the gap structure using quasiparticle interference imaging, where it was suggested that the results are most consistent with $d_{x^2-y^2}$ symmetry, similar to that of the cuprates[64]. Such a lack of TRS breaking was concluded from a recent study of Josephson junctions formed between Sr_2RuO_4 and Nb, due to the invariance of the Josephson critical current upon reversing the current and field directions[65]. On the other hand, as mentioned above the μSR evidence for TRS breaking has been backed up by optical Kerr effect measurements[21]. Moreover, a recent μSR study of Sr_2RuO_4 under uniaxial stress again confirmed the enhancement of the μSR relaxation rate below T_c in unstressed samples[66]. Interestingly, the application of uniaxial stress appears to decouple the onset of TRS breaking from the superconducting transition, where there is a slight decrease of the onset temperature with increasing stress, while T_c increases. Evidence for a two-component

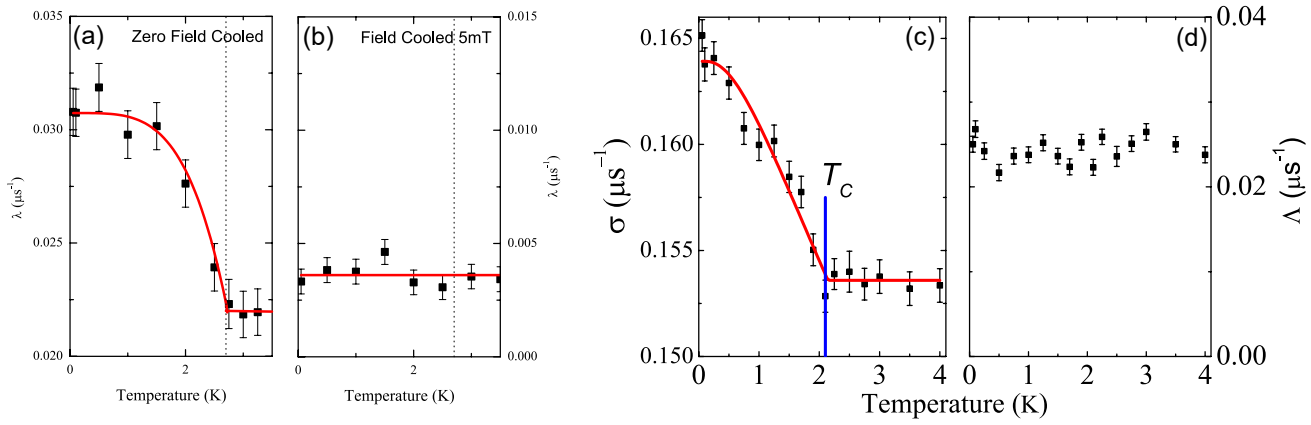

FIG. 2. Lorentzian relaxation rate λ_{ZF} obtained from fitting μSR spectra of $LaNiC_2$ in (a) zero-field, and (b) a longitudinal field of 5 mT. In zero-field there is a clear increase of λ_{ZF} correlated with T_c, which disappears in the longitudinal field. Reproduced with permission Ref. 11. Copyright 2009 by the American Physical Society. From the analysis of the zero-field μSR of $LaNiGa_2$, the temperature dependence of the (c) the Gaussian relaxation rate σ_{ZF}, and (d) the Lorentzian relaxation rate Λ are displayed. In this case σ_{ZF} shows a clear increase below T_c, while Λ remains unchanged. Reproduced with permission Ref. 13. Copyright 2012 by the American Physical Society.

TABLE II. A list of those strongly correlated superconductors where μSR or the Kerr effect have been used to provide evidence for either the presence or absence of time-reversal symmetry in the superconducting state.

Material	Broken TRS?	Reference
UPt_3	✓/×	22,38,44
UBe_{13}	×	32
$U_{1-x}Th_xBe_{13}$ $(0.02 \leq x \leq 0.04)$	✓	32
URu_2Si_2	✓	23
UTe_2	✓	41
$CeCu_2Si_2$	×	45
$CeCoIn_5$	×	46
$CeIrIn_5$	×	46
$YBa_2Cu_3O_7$	×	47,48
$Bi_2Sr_{2-x}La_xCuO_{6+\delta}$	×	47,49
$Ba_{1-x}K_xFe_2As_2$	×,✓$(0.7 \lesssim x \lesssim 0.85)$	50–52
Sr_2RuO_4	✓	21,33
$Pr(Os_{1-x}Ru_x)_4Sb_{12}$	✓	53,54
$Pr_{1-y}La_yOs_4Sb_{12}(y<1)$	✓	54
$Pr_{1-y}La_yPt_4Ge_{12}(y<1)$	✓	55,56

order parameter has also been reported from two studies, based on a discontinuity in the shear elastic modulus c_{66} at T_c[67,68]. It was pointed out that both a chiral $d_{xz}+id_{yz}$ state, and an accidentally degenerate $d_{x^2-y^2}+ig_{xy(x^-y^2)}$ state corresponding to a mixture of representations, are compatible with the requirements of a multicomponent singlet order parameter with broken TRS. However, further studies are still required to determine the nature of the pairing state, and resolve the apparent discrepancies between the results of different measurement techniques.

It should be noted that TRS breaking is by no means an ubiquitous feature of strongly correlated unconventional SCs (Table II). In addition to the aforementioned stoichiometric UBe_{13}[32], a lack of evidence for TRS breaking is also found from μSR measurements of the heavy fermion SCs $Ce(Co,Ir)In_5$[46] and $CeCu_2Si_2$[45]. Meanwhile, zero-field μSR measurements do not reveal evidence for broken TRS in the superconducting states of the high-T_c cuprates $YBa_2Cu_3O_7$ (YBCO) and $Bi_2Sr_{2-x}La_xCuO_{6+\delta}$[47–49], as expected for $d_{x^2-y^2}$ symmetry (although evidence for a spontaneous magnetization below T_c was reported from SQUID measurements of YBCO films[69]). We note however, that TRS breaking has been detected in the normal state of underdoped cuprates[70,71], which is associated with the pseudogap phase. In the case of the Fe-based SCs, optimally doped $Ba_{1-x}K_xFe_2As_2$ ($x \approx 0.6$) has been widely suggested to have a nodeless sign-changing $s_\pm$ pairing state[72–75] while heavily hole doped KFe_2As_2 was proposed to be a nodal d-wave SC[76–79]. It was predicted that the crossover between these pairing states with different symmetries should be via an intermediate $s+id$ state with broken TRS[80]. Experimentally, an initial zero-field μSR study of a number of dopings in the range $x = 0.5-0.9$ found no evidence for TRS breaking[50]. Meanwhile, another μSR study of a crystal with doping $x \approx 0.73$, which was ion-irradiated so as to create lattice symmetry breaking defects, showed evidence for TRS breaking in the superconducting state[51]. The different results from the previous study was attributed to the $s+id$ state existing only

over a narrow doping range. However, subsequent studies suggested that s-wave pairing symmetry is preserved across the entire $Ba_{1-x}K_xFe_2As_2$ phase diagram, even in the nodal states of the heavily hole doped samples[81,82]. Recently, μSR measurements identified the presence of a region with broken TRS for $0.7 \lesssim x \lesssim 0.85$[52], which the authors proposed corresponds to a dome-like $s + is$ state separating the two distinct TRS preserving s-wave phases. The $s + is$ phase was identified as occuring just beyond a doping induced Lifshitz transition, at which the electron pockets drop below the Fermi level[83]. They found the spontaneous fields below T_c to be anisotropic, predominantly being polarized within the ab-plane. This is the anticipated behavior for the $s+is$ state in the presence of sample inhomogeneities, whereas for the $s + id$ state the ab-plane and c-axis components are expected to be of similar magnitudes[84].

B. Rare-earth based filled-skutterudites

The filled-skutterudites MT_4X_{12} (M = rare earth or alkaline earth, T = transition metal, and X = Ge, P, As, Sb) are a large family of materials with fascinating properties, in which several compounds become superconducting at low temperature[85–89]. Among these, the heavy fermion SC $PrOs_4Sb_{12}$ is unique in that superconductivity is likely mediated by quadrupolar fluctuations[87]. On the other hand, other filled skutterudite SCs behave more like conventional s-wave SCs[90–93], lacking evidence for strong electronic correlations. TRS breaking has been found from zero-field μSR measurements of $PrOs_4Sb_{12}$[53] and $PrPt_4Ge_{12}$[55]. In the case of $PrOs_4Sb_{12}$, this conclusion was also supported by Kerr effect measurements[25]. The TRS breaking appears to be related to the presence of Pr^{3+} ions, since the size of the increase in $\sigma_{\rm ZF}$ below T_c is reduced by La-doping, and TRS breaking is not detected in the purely La-based compounds[54,56]. Furthermore, a more rapid suppression of TRS breaking is observed when replacing Os with Ru atoms in $PrOs_4Sb_{12}$[54].

The superconducting properties of MT_4X_{12} have been intensively studied, in particular for the compounds $PrOs_4Sb_{12}$ and $Pr_xPt_4Ge_{12}$, but the nature of their order parameter remains to be established. A number of measurements, including measurements of the lower critical field, thermal conductivity and μSR suggest fully gapped multiband superconductivity for these compounds[94–99]. However, there are also signatures of unconventional superconductivity in $PrOs_4Sb_{12}$, such as the absence of a coherence peak in $1/T_1$ below T_c[100], as well as evidence for point nodes from the penetration depth[101] and angular dependent thermal transport[102]. Substitution of either Pr by La, or Os by Ru in $PrOs_4Sb_{12}$ leads to the suppression of the nodal behavior, suggesting a possible change of the pairing state in the doped compounds[54,56,103]. Similar debate also exists for $PrPt_4Ge_{12}$. The early measurements of the specific heat and μSR suggest nodal superconductivity for $PrPt_4Ge_{12}$[104]. Later measurements of the London penetration depth[105,106], specific heat, thermal transport[92], NQR[107] and photoemission spectroscopy[108] demonstrate that both $PrPt_4Ge_{12}$ and $LaPt_4Ge_{12}$ behave more like conventional BCS SCs with a fully opened energy gap. The smooth evolution of the superconducting transition between the Pr-based end compounds with TRS breaking, and the time reversal preserving La-based materials, is difficult to account for and requires further studies.

C. TRS breaking in fully gapped superconductors

In recent years there have been a number of reported cases of materials with evidence for TRS breaking in the superconducting state, which appear to be quite distinct from the aforementioned examples in strongly correlated SCs. The properties of these systems are also in Table I. Besides there being a lack of evidence for an underlying correlated state in many cases, the superconducting properties generally appear to behave similar to conventional s-wave SCs, i.e. the superconducting gap is fully open over the whole Fermi surface. This leads to the question of whether the origin of TRS breaking is from an unconventional superconducting state arising from a pairing mechanism other than the electron-phonon mechanism of BCS theory, or if such behavior can be realized via conventional pairing.

1. *$LaNiC_2$ and $LaNiGa_2$*

Evidence for TRS breaking has been found from zero-field μSR measurements of the SCs $LaNiC_2$ (T_c = 2.7 K)[11] and $LaNiGa_2$ (T_c = 2.1 K)[13]. These materials crystallize in different, but related orthorhombic crystal structures. $LaNiGa_2$ crystallizes in a centrosymmetric structure with space group $Cmmm$ (point group D_{2h})[109], whereas $LaNiC_2$ has a noncentrosymmetric space group $Amm2$ (point group C_{2v}), where inversion symmetry is broken within the Ni-C layer lying half way between the A-faced centers[110]. The TRS breaking is manifested by an abrupt increase in the relaxation rate of the asymmetry in the zero-field μSR spectra measured below T_c, while above T_c, the spectra are temperature independent (Fig. 2). Upon analysis using Eq. 4, it was found that the increase below T_c is in $\lambda_{\rm ZF}(T)$ for $LaNiC_2$, but $\sigma_{\rm ZF}(T)$ for $LaNiGa_2$. Since however, the effect is destroyed in $LaNiC_2$ by the application of a small longitudinal field of 5 mT, the behavior for both compounds was ascribed to the spontaneous onset of weak static fields in the superconducting state.

In $LaNiC_2$, the occurrence of TRS breaking is supported by magnetization measurements using a SQUID magnetometer[34]. Here single crystalline $LaNiC_2$ was measured together with a reference SC Ta, where the latter was used to detect and cancel the stray field.

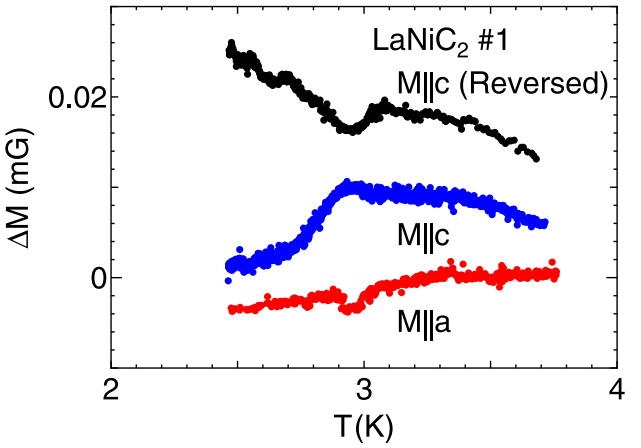

FIG. 3. Temperature dependence of the magnetization change $\Delta M(T)$ of $LaNiC_2$ measured upon cooling below T_c in zero-field, with respect to the data at 3.5 K. A clear increase in $\Delta M(T)$ is observed below T_c, while when the sample direction is reversed, there is also a sign change of $\Delta M(T)$, suggesting the spontaneous occurrence of a bulk magnetization. Reproduced with permission from Ref. 34. Copyright 2015 by the Physical Society of Japan.

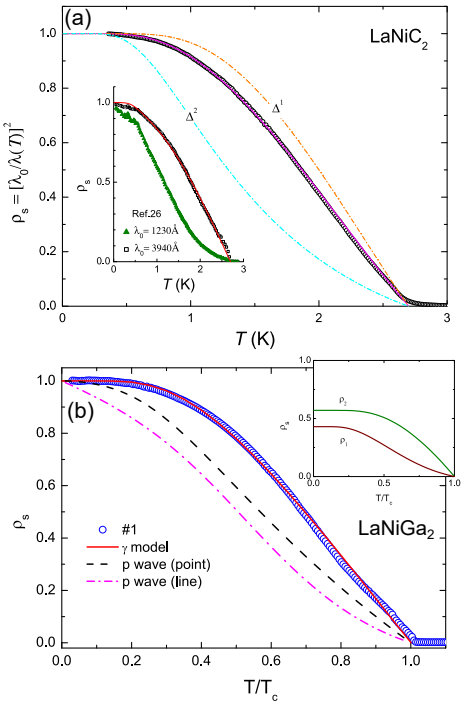

FIG. 4. (a) Temperature dependence of the normalized superfluid density, derived from $\Delta\lambda(T)$ measured using the tunnel-diode oscillator based technique for (a) $LaNiC_2$, and (b) $LaNiGa_2$. The solid lines in both panels show the results from fitting using nodeless two-gap models. Panel (a) is reproduced from Ref. 112, available under a Creative Commons Attribution 3.0 Unported (CC-BY) license. (b) is reproduced with permission from Ref. 14. Copyright 2016 by the American Physical Society.

The zero-field magnetization of $LaNiC_2$ was then determined by measuring the magnetic flux change upon cooling under these zero-field conditions. Figure 3 shows the temperature dependence of the magnetization change $[\Delta M(T)]$ for the highest quality crystal, after subtracting the value at 3.5 K. It can be seen that while no features occur along the a-axis, there is a distinct increase of $\Delta M(T)$ along the c-axis. Moreover, when the sample direction is reversed, the sign of ΔM is also flipped, suggesting that this magnetization is intrinsic to the sample. While in TRS breaking SCs, the presence of differently orientated domains may be expected to lead to zero net magnetization (as opposed to the local magnetic fields detected using μSR), the authors suggest that the lack of equivalence between the [001] and [00$\bar{1}$] directions in the noncentrosymmetric crystal structure may lead to pinning of the magnetization along this direction.

The superconducting gap structures of both materials have been probed via a number of methods. While initially a T^3 dependence of the specific heat was reported for $LaNiC_2$[110], suggesting a line nodal gap, subsequent measurements at low temperatures reported the exponential behavior characteristic of a fully open gap[111,112]. This conclusion was corroborated by penetration depth measurements using the tunnel-diode oscillator based technique[112], as well as a nuclear quadrupole resonance (NQR) study of the spin-lattice relaxation rate[113]. Meanwhile fully-gapped superconductivity in $LaNiGa_2$ was reported from measurements of both the specific heat and magnetic penetration depth[14,109]. Moreover, from combining low temperature magnetic penetration depth measurements performed using the tunnel-diode oscillator based method, specific heat and upper critical field results, it was found that the behaviors of both compounds are consistently well described by a model with two nodeless gaps (Fig. 4)[14,112], indicating that nodeless two-gap superconductivity is another common feature of $LaNiC_2$ and $LaNiGa_2$. These experimental results were reconciled by the proposal of an internally-antisymmetric nonunitary triplet ground state, described in more detail in Section VII.

2. *Noncentrosymmetric La_7X_3 and ReX*

In noncentrosymmetric SCs, antisymmetric spin-orbit coupling (ASOC) can give rise to a mixed singlet-triplet pairing state. As discussed in Section VII, however, the low symmetry of the orthorhombic point group of $LaNiC_2$ means that even if inversion symmetry is broken, the ASOC cannot give rise to mixed singlet-triplet pairing states which break time-reversal symmetry at T_c. On the other hand, TRS breaking has been found in several other noncentrosymmetric SCs with higher symmetries, which opened up the possibility for such singlet-triplet mixing.

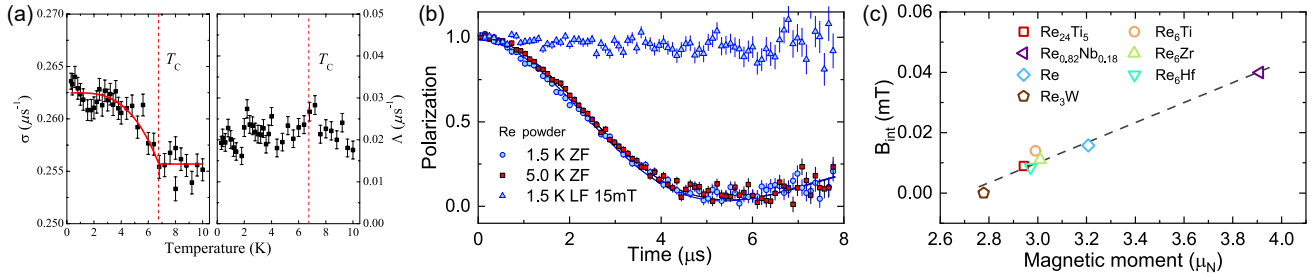

FIG. 5. (a) Temperature dependence of the Lorentzian and Gaussian relaxation rates obtained from zero-field μSR measurements of Re_6Zr, where the latter shows a clear increase below T_c indicating TRS breaking. Reproduced from Ref. 114, available under a Creative Commons Attribution 3.0 License. (b) μSR time spectra of elemental Re measured in zero-field above and below T_c, and in a longitudinal field of 15 mT in the superconducting state. The more rapid depolarization below T_c indicates the presence of TRS breaking of elemental Re, and as shown in the inset this onsets below T_c. (c) Plot of the internal field estimated from the increase of σ_{ZF} below T_c as a function of the nuclear moment calculated from the nuclear moments of the constituent elements and their relative fractions. A clear positive correlation is observed between the two quantities. Both (b) and (c) are reproduced with permission from Ref. 115. Copyright 2018 by the American Physical Society.

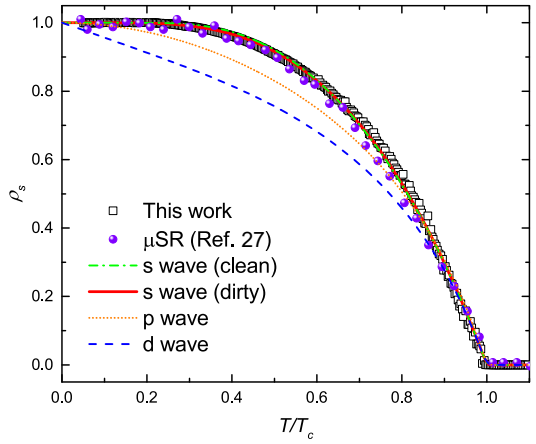

FIG. 6. Temperature dependence of the superfluid density of Re_6Zr, derived from measurements of the magnetic penetration depth using the tunnel-diode oscillator based method. The superfluid density determined from μSR measurements are also displayed[114], where close agreement is found from the two methods. The data are well described by single gap isotropic s-wave models for both the clean and dirty limits. Reproduced with permission from Ref. 116. Copyright 2018 by the American Physical Society.

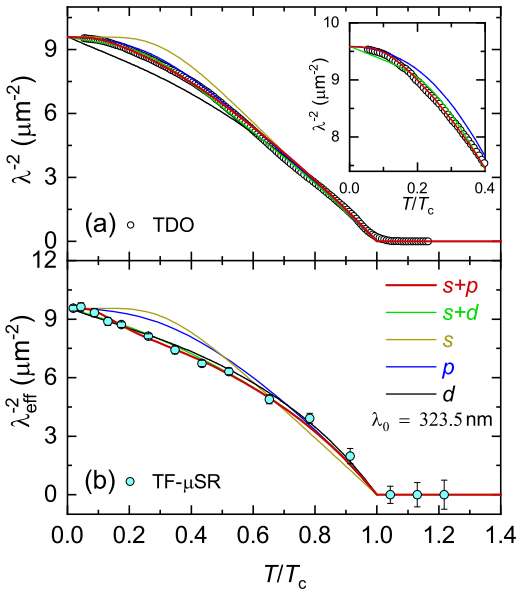

FIG. 7. Temperature dependence of the superfluid density of CaPtAs, derived from measurements of the magnetic penetration depth using the (a) tunnel-diode oscillator based method, and (b) transverse field μSR. In both cases the superfluid density is best described by a two-gap $s+p$ model, which has one fully open and one nodal gap. Reproduced with permission from Ref. 117. Copyright 2020 by the American Physical Society.

La_7Ir_3 and La_7Rh_3 crystallize in the noncentrosymmetric hexagonal Th_7P_3 type-structure with T_c = 2.3 and 2.65 K, respectively. Zero-field μSR on La_7Ir_3 revealed a clear increase of $\lambda_{ZF}(T)$ below T_c, similar to the case of $LaNiC_2$, while σ_{ZF} shows little change[118]. Meanwhile from μSR measurements in an applied transverse field, the temperature dependence of the superfluid density derived from the magnetic penetration depth $\lambda(T)$ is very well described by a single isotropic gap, with a magnitude slightly larger than that of weak coupling BCS theory[118]. The good accordance with single gap s-wave superconductivity is also supported by the analysis of the specific heat[119]. Furthermore, the estimated T_c based on a first principles calculation of the phonon frequencies and electron phonon-coupling constant is very close to the experimentally observed value, giving a strong indication of a conventional electron-phonon pairing mechanism[119]. Evidence for TRS breaking was also found in La_7Rh_3, where the penetration depth could be described by a single band s-wave model[120].

Another large class of materials where evidence for TRS breaking superconductivity is found is in Re-based alloys ReX with the α-Mn type cubic structure (space group $I\bar{4}3m$), which were first reported by Matthias *et al.* nearly 60 years ago[121,122]. The crystal structure has a large unit cell with 58 atoms and four distinct crystallographic sites. These systems are generally non-stoichiometric with intrinsic site disorder, especially on the two sites with 24g Wyckoff positions. TRS breaking below T_c was initially found from μSR measurements of Re_6Zr[114], as displayed in Fig. 5. Here the symmetry analysis for the cubic point group shows that TRS breaking singlet-triplet mixing pairing states below T_c are permitted. TRS breaking was subsequently reported in several other ReX systems including Re_6Hf[123], Re_6Ti/$Re_{24}Ti_5$[124,125] and $Re_{0.82}Nb_{0.18}$[115]. In all cases, the TRS breaking is manifested by the increase of $\sigma_{\rm ZF}$ below T_c. Moreover, while some studies have found evidence for two-gap superconductivity in ReX[126,127], most measurements were generally well accounted for by a single gap s-wave model[114–116,123–125,128–134]. An example of this is displayed in Fig. 6, where it can be seen that the superfluid density derived from penetration depth measurements of single crystals of Re_6Zr using the tunnel diode oscillator based method are well described using a model with a single isotropic gap[116]. Furthermore, these data are highly consistent with the superfluid density determined from transverse field μSR results[114].

A very surprising result was however reported in Ref. 115, which shows that the element rhenium also exhibits the signatures of TRS breaking in the superconducting state [Fig. 5(b)]. Rhenium has a simple centrosymmetric crystal structure, and this therefore suggests that the breaking of inversion symmetry and the accompanying ASOC are not crucial ingredients for realizing TRS breaking in this series. This rather suggests that the local electronic structure of Re is important. This is consistent with α-Mn type SCs which do not contain Re but still have sizeable ASOC, such as $Nb_{0.5}Os_{0.5}$ and $Mg_{10}Ir_{19}B_{16}$, being found not to exhibit TRS breaking[135,136]. Furthermore, as shown in Fig. 5(c) a clear correlation is found between the magnitude of the internal field emerging below T_c, which can be estimated from the increase of $\sigma_{\rm ZF}$, and the size of the nuclear moments μ_n corresponding to $\mu_{\rm n} = \sqrt{f_{\rm Re}\mu^2_{\rm n,Re} + f_X\mu^2_{\rm n,X}}$, where $\mu_{\rm n,Re}$ and $\mu_{\rm n,X}$ are the nuclear moments of Re and X elements, and f are the relative fractions. Since $\mu_{\rm n,Re}$ is relatively large, the systems with larger Re content generally show a larger internal field, while in less Re rich Re_3W, TRS breaking cannot be detected[137]. However the origin of this correlation is difficult to account for, and this requires further experimental and theoretical study.

3. *Equiatomic arsenides SrPtAs and CaPtAs*

Although most of the recent examples of SCs with broken TRS have been noncentrosymmetric systems, the role played, if any, by the broken inversion symmetry in giving rise to this phenomenon remains to be established. The crystal structure of SrPtAs is globally centrosymmetric, with the hexagonal space group $P6_3/mmc$, and it becomes superconducting below $T_c = 2.4$ K[138]. However, the structure consists of two Pt-As layers stacked alternately along the c-axis, where inversion symmetry is broken locally within the layers. Therefore if the coupling between Pt-As layers is weak, novel superconducting pairing states may be realized[139], similar to the case where inversion symmetry is globally absent. TRS was found to be broken below T_c in SrPtAs from an increase of $\lambda_{\rm ZF}$ below T_c[137]. Despite a number of novel theoretical proposals such as chiral d-wave and f-wave pairings[140–142], Knight shift measurements indicate the presence of singlet pairing[143], and probes of the gap structure can be accounted for with a nodeless isotropic gap[137,143–145].

CaPtAs is superconducting below $T_c = 1.47$ K[146], and has a noncentrosymmetric tetragonal structure consisting of a three-dimensional hexagonal network of Pt-As atoms, with the same chiral space group ($I4_1md$) as a number of equiatomic ternary SC's RTX (R=La or Th, T=transition metal, X=Si, Ge, As or P)[147–154]. The structure of CaPtAs however is different from the LaPtSi-type structure of the latter compounds, having a greatly elongated c-axis which is about three times longer[155].

Evidence for broken TRS in CaPtAs is also found from zero-field μSR measurements, due to an increase of $\lambda_{\rm ZF}$ below T_c[117]. However as displayed in Fig. 7, the superfluid density derived from both transverse-field μSR and the tunnel-diode oscillator based technique does not saturate at low temperatures, indicating a nodal superconducting gap, which is corroborated by the analysis of the specific heat[117,146]. This is in contrast to the behavior of other noncentrosymmetric SCs with broken TRS, which have generally been found to have nodeless gaps. The superfluid density data are best described by a two-gap model with one fully open gap, and another with point nodes[117]. These results suggest the possibility of mixed singlet-triplet pairing together with broken TRS, but confirmation of this scenario requires further theoretical and experimental studies.

4. *$R_5Rh_6Sn_{18}$*

The $R_5Rh_6Sn_{18}$ (R=Lu, Y, Sc) SCs have a centrosymmetric caged structure[156]. Here the tetragonal structure with space group $I4_1/acd$ corresponds to a distortion of a cubic structure, where the periodicity of the lattice doubles along the c-axis. The signatures of TRS breaking were found for all three compounds from zero-field μSR measurements[157–159], as manifested in an increase

of λ_{ZF} below T_c. On the basis of a symmetry analysis, two potential unconventional TRS breaking states were proposed, a $d+id$ singlet state and a non-unitary triplet state[157]. The former has two point nodes and a line node on a three-dimensional Fermi surface, while the latter has only point nodes. On the other hand, the superfluid density extracted from transverse field μSR measurements for R=Lu and Y saturates at low temperature, and is well described by a single isotropic gap[157,158]. Moreover, nodeless superconductivity was deduced for these two compounds from the absence of a residual contribution to the thermal conductivity at low temperatures[160], while the specific heat of $Sc_5Rh_6Sn_{18}$ is also well described by an s-wave model[161]. However, in the case of $Y_5Rh_6Sn_{18}$ evidence for gap anisotropy was found from a four-fold oscillation of the specific heat coefficient in the ab-plane[162], and a non-linear field dependence of the same quantity[163], suggesting a possible deviation from isotropic s-wave superconductivity.

IV. THEORETICAL ANALYSIS

In this section, we outline theoretical efforts to understand the order parameter symmetry and underlying pairing mechanisms of the TRS breaking SCs discussed in the previous section. The starting point is the group-theoretical formulation of Ginzburg-Landau (GL) theory[164–166]. This very general technique allows us to obtain important information about the superconducting ground state using only general symmetry properties of the material, that is, without requiring information about the underlying pairing mechanism. Once this has been achieved, the experimentally observable properties of the symmetry-allowed ground states can be investigated by a generalized BCS-type mean-field approach within the Bogoliubov-de Gennes formalism[166]. This second step may require a model for the pairing interaction. We describe applications of such approaches to the materials discussed above, emphasizing how experimental data, band structure and such theories can in principle lead to a complete understanding of the properties of the TRS-breaking superconducting ground states. We also discuss the difficulties that are encountered in practice in trying to carry out such a programme.

A. Group theoretical formulation of the Ginzburg-Landau theory

Here we review the group theoretical formulation of the GL theory used to constrain possible forms of superconducting order parameters using the underlying symmetries of the crystal structure without requiring the knowledge of the pairing mechanisms. We use specific examples of TRS breaking superconducting materials to illustrate what can be learned about possible order parameters based on these general considerations. In particular, we discuss the conditions under which TRS breaking implies symmetry-required nodes on the Fermi surface in view of their respective band structures and the constraints on the pairing state imposed by spin-orbit coupling depending on the presence of inversion symmetry in the SCs.

Landau theory[167] is a phenomenological theory of continuous phase transitions. It has been immensely successful in accurately predicting the qualitative features of a wide range of phase transitions featuring change in symmetry. The basic assumption of the theory is that there is a continuous transition at a given transition temperature (T_c), between symmetrically distinct low temperature and high temperature phases. The aim is to establish a relation between the symmetries of the two phases and find relevant physical thermodynamic quantities which change anomalously across the transition. This is achieved by introducing the concept of an order parameter and a thermodynamic potential. The change in symmetry across the phase transition is quantified by the order parameter, a thermodynamic quantity (e.g. magnetization of a ferromagnet) which is zero in the symmetric (disordered) high temperature phase and nonzero in the ordered phase at low temperatures. Since the transition is assumed to be continuous, the absolute size of the order parameter can be assumed to be small near T_c such that the thermodynamic potential can be expressed as a Taylor expansion of the order parameter components and only one irreducible degree of freedom participates in determining the symmetry breaking at T_c. Important consequences are discontinuous changes in physical quantities related to second-order derivatives of the thermodynamic potential at T_c and the absence of co-existent regions of two phases.

We now focus on the case of a superconducting phase transition. From the point of view of GL theory, the superconducting phase transition is a continuous phase transition accompanied by spontaneous gauge symmetry breaking at T_c. The latter leads to the rigidity of the phase of the electron fluid which in turn gives rise to the classic properties of SCs: zero resistance, Meissner effect and the Josephson effect[168].

B. Normal state symmetry group

In discussing the symmetry properties of the possible superconducting order parameters we first need to consider the generic symmetry properties of the material. In the normal state, the system must be invariant under the normal state symmetry group[164–166] defined as

$$\mathcal{G} = G \otimes U(1) \otimes \mathfrak{T}. \tag{7}$$

Thus $\mathcal{G}$ is a direct product (represented by $\otimes$) group of the group G of crystalline symmetries with rotations in spin space, the gauge symmetry group $U(1)$ and the group of time reversal operations $\mathfrak{T}$. When spin-orbit coupling (SOC) is not important and the normal state is nonmagnetic, we can write $G = G_c \otimes SO(3)$ where G_c is

the space group of the crystal and $SO(3)$ is the group of rotations in spin space in 3D.

Landau theory states that the possible symmetries of the order parameter just below T_c are determined by the irreducible representations (irreps) of G. Near T_c, the GL free energy can be approximated by a finite Taylor expansion in the order parameter components as the magnitude of the order parameter itself is small. The free energy thus expressed must be invariant under G. Remarkably, this is enough to constrain the possible symmetries of the order parameter. SCs which only break the $U(1)$ symmetry are called conventional SCs and those with additional broken symmetries other than $U(1)$ are termed, in this context, unconventional SCs.

We will consider superconducting instabilities that are uniform throughout the system. In this case, the possible superconducting order parameters can be constructed by considering only the symmetries of a single unit cell. For a crystal with symmorphic space group, the symmetry of a unit cell is described by the point group (containing rotations and reflections) of the underlying Bravais lattice. In this case, we can write $G_c = G_0 \otimes T$ where T is the translation group of the crystal and G_0 is the crystalline point group. However, for a crystal with nonsymmorphic space group symmetries the symmetry operations within a unit cell include nonsymmorphic operations such as screw axes (rotation about an axis with a fractional translation, i.e. by a fraction of the primitive lattice vector, parallel to the axis of rotation) and/or glide planes (reflection in a plane followed by a fractional translation parallel with that plane). These are in addition to some of the regular point symmetry operations.

The presence of nonsymmorphic symmetries has important consequences for the gap structure of a material which include the violation of Blount's theorem[169]. Blount's theorem states that no symmetry protected line nodes are allowed in an odd-parity SC. Although symmorphic crystals obey this theorem, recent studies[170–173] have shown that nonsymmorphic symmetries can lead to symmetry protected line nodes even in odd-parity SCs. The essence is that the nonsymmorphic symmetries can cause additional symmetry-required nodes on the Brillouin zone faces along high-symmetry directions. These nodes will affect the thermodynamic properties of the system when Fermi surfaces touch the Brillouin zone edges *and* are not "open" along those high-symmetry directions. Barring these symmetry-required nodes, the overall symmetry of the order parameter can still be determined by considering the underlying point group operations of the crystal. This is the approach we take in the following discussions.

C. Construction of the GL free energy

Under the general assumptions of Landau theory, i. e. the existence of an order parameter and its continuous change as a function of temperature across T_c, we can construct a generic form valid near T_c of the GL free energy as a Taylor expansion of the order parameter. In this regime, the order parameter and its spatial variation is assumed to be small. Taking the order parameter to consist of a set of complex numbers $\{\Delta_i\}$ which will vary continuously as functions of T and vanish when $T > T_c$, the generic form of the GL free energy[165,166] in the absence of magnetic fields is given by

$$f = f_0 + \sum_{i,j} \Delta_i^* \alpha_{i,j} \Delta_j + \sum_{i,j,k,l} \Delta_i^* \Delta_j^* \beta_{i,j,k,l} \Delta_k \Delta_l + \sum_{i,j,k,l} \partial_i \Delta_j^* \mathcal{K}_{i,j,k,l} \partial_k \Delta_l + \dots \quad (8)$$

Here, f_0 is the free energy of the normal state, $\alpha_{i,j}$ are the elements of the inverse pairing susceptibility matrix $\hat{\alpha}$, $\beta_{i,j,k,l}$ are the elements of the $\hat{\beta}$ tensor characterizing the fourth order term and $\mathcal{K}_{i,j,k,l}$ are the elements of the $\hat{\mathcal{K}}$ tensor characterizing the spatial variation of the free energy. The free energy has the same symmetry as an effective action or an effective Hamiltonian describing the normal state and must be invariant under the transformations of the normal state symmetry group $\mathcal{G}$. As a result, the way the order parameter changes under the operations in $\mathcal{G}$ implies that the elements of $\hat{\alpha}$, $\hat{\beta}$ and $\hat{\mathcal{K}}$ are constrained by symmetry. For example, 1) the free energy must be real and invariant under TRS which constrains $\hat{\alpha}$ to be a real symmetric matrix and $\hat{\beta}$ to be a real tensor, 2) $\beta_{i,j,k,l} = \beta_{j,i,k,l} = \beta_{i,j,l,k} = \beta_{j,i,l,k}$, 3) free energy has to be invariant under G which implies $\hat{\alpha} = \hat{R}_g^\dagger \hat{\alpha} \hat{R}_g \ \forall g \in G$ with $\hat{R}_g$ being a matrix representation of the element g.

Representation theory of groups can now be used to block-diagonalize the $\hat{\alpha}$ matrix with blocks of the same dimensions as those of the irreps of G. Each block can further be transformed, using a suitable basis for the irrep of dimension d, into a number times the identity matrix of order d. Thus a d-dimensional irrep produces a d-fold degenerate eigenvalue. These eigenvalues of the $\hat{\alpha}$ matrix are of special significance since they correspond to all the possible symmetry allowed channels of superconducting instabilities in the system.

At high temperature the superconducting state is unstable, leading to all the eigenvalues being positive definite. But as the temperature is lowered, they can change sign. Assuming the eigenvalue α_1 changes sign first, we can take the form $\alpha_1 = a_0(T - T_c)$ with a_0 being a positive real number. The analyticity of α_1 stems from the basic underlying assumption of continuous change of the order parameter as a function of temperature. The instability corresponding to α_1 will have the highest T_c and will characterize the superconducting properties of the ground state of the system.

We consider the instability with the highest T_c to correspond to the d-dimensional irrep Γ of G. Then the corresponding order parameter of the system close to T_c

can be written as

$$\hat{\Delta}(\boldsymbol{k}) = \sum_{m=1}^{d} \eta_m^{\Gamma} \Delta_m^{\Gamma}(\boldsymbol{k}) \tag{9}$$

where η_m^{Γ} are the complex amplitudes of the order parameter $\hat{\Delta}$, also called the gap matrix or the pairing potential, corresponding to the basis functions $\Delta_m^{\Gamma}(\boldsymbol{k})$ of Γ. The thermodynamic properties of the state are then completely described by the set $\{\eta_m^{\Gamma}\}$ and thus those amplitudes can be used as an alternative description of the order parameter. In the basis function space $\{\Delta_m^{\Gamma}(\boldsymbol{k})\}$, these numbers transform as: $\mathcal{T}\eta = \eta^*$ and $\mathcal{C}\eta = e^{i\phi}\eta$ where $\mathcal{T}$ is the TRS operator and $\mathcal{C}$ is the gauge transformation operator with ϕ being a phase.

We now restrict our discussion to the particular irrep Γ and write the free energy as a Taylor expansion in $\{\eta_m\}$ (dropping the Γ label):

$$f = f_0 + a_0(T - T_c)\sum_m |\eta_m|^2 + \sum_{ijkl} \beta_{ijkl}\eta_i^*\eta_j^*\eta_k\eta_l + \sum_{ijkl} \mathcal{K}_{ijkl}\partial_i\eta_j^*\partial_k\eta_l + \dots \tag{10}$$

For overall stability, the fourth order term in the free energy must be positive definite. The terms corresponding to a particular order in the free energy can now be constructed by constructing invariant polynomials[164–166] of that order corresponding to the particular irrep of the symmetry group. Thus the symmetry constraints result in a fourth order term which depends on a few, material-dependent parameters $\{\beta_n\}$. By minimizing the free energy for $T < T_c$ with respect to all the complex variables $\{\eta_i\}$, all the distinct superconducting states that can exist just below T_c for an instability in the channel Γ can now be obtained and a phase diagram showing which of these states is realized depending on the values of the GL parameters can be constructed. In each of the phases there will be a particular relation between the different η_i coefficients. If their complex phases differ by more than a mere change of sign, then we have a state with broken TRS. Evidently this requires a degenerate instability channel, i.e. one with $d > 1$.

It is worth noting that following the above procedure we may still find that some of the states in a given channel are degenerate. The degeneracy can be lifted[166] by the effects of crystal field splitting, SOC and/or strong coupling. Mostly, the fourth order term in the free energy is sufficient to get non-degenerate superconducting states when crystal field, SOC or strong coupling effects are taken into account. However, in some cases, a few spurious degeneracies can still remain requiring the need to consider higher order terms[166] in the free energy. We will only consider the free energy up to fourth order in the subsequent discussions. One important point to note is that classifying the superconducting states in this manner gives emphasis only on the symmetry of the order parameter and not on its specific form.

D. Structure of the order parameter

In determining the structures of the possible order parameters, it is important to consider the effect of SOC on the normal state band structure of the material. If SOC leads to significant band splitting near the Fermi level, most probably it will be important in determining the properties of the superconducting ground state. If we consider BCS-type pairing in an effective single band picture, the Cooper pairs can only be of two types: spin singlet and spin triplet. These two kinds of pairing, singlet and triplet, can be distinguished by their different behaviors under rotations in spin space in the absence of SOC or when the effect of SOC can be neglected. But when SOC is finite and cannot be neglected, spin rotation and space rotation cannot be separated. Then, since the overall Cooper pair wave function has to be antisymmetric, only parity ($\hat{P}$) of the Cooper pair wave function can distinguish between spin singlet (even parity) and spin triplet (odd parity) states.

The above argument applies to any centrosymmetric SC. However, a noncentrosymmetric material lacks inversion symmetry. As a result, parity is not a well defined symmetry in this case. The crucial difference between centrosymmetric and noncentrosymmetric SCs is that for noncentrosymmetric SCs the irreps of G_0 do not have distinct symmetries under inversion and thus each of them are compatible with both singlet and triplet pairing. This results in the admixture of singlet and triplet pairing within the same superconducting state of a noncentrosymmetric material with strong SOC[174]. In contrast, centrosymmetric SCs have either purely singlet or purely triplet pairing even with strong SOC, distinguishable by their respective parities. Thus noncentrosymmetric SCs are in this sense special since SOC has more dramatic effect on them than in their centrosymmetric counterparts.

In the case of strong SOC, the single-particle states are no longer the eigenstates of spin and we need to label them rather by pseudospins. The pseudospin states are linear combinations of the spin eigenstates. However, the pseudospin states can be thought to be generated from the spin eigenstates by adiabatically turning on the SOC. Hence, the original spin eigenstates and the pseudospin states have one-to-one correspondence. If α and β labels the pseudospin states then we can identify $\uparrow\equiv\ \alpha$ and $\downarrow\equiv\ \beta$. In such a system zero momentum Cooper pairs are formed from particles from energetically degenerate states. The pseudospin states $|\boldsymbol{k},\alpha\rangle$ and its time reversed partner $\mathcal{T}|\boldsymbol{k},\alpha\rangle = |-\boldsymbol{k},\beta\rangle$ (where $\mathcal{T}$ is the time-reversal operator) are paired for the case of even parity singlet pairing while four degenerate states $|\boldsymbol{k},\alpha\rangle$, $\mathcal{T}|\boldsymbol{k},\alpha\rangle = |-\boldsymbol{k},\beta\rangle$, $\mathcal{P}|\boldsymbol{k},\alpha\rangle = |-\boldsymbol{k},\alpha\rangle$ and $\mathcal{TP}|\boldsymbol{k},\alpha\rangle = |\boldsymbol{k},\beta\rangle$ ($\mathcal{P}$ is the parity or the inversion operator) participate in pairing in the case of odd parity pairing. Since the pseudospin and the spin are closely related, the even parity states correspond to pseudospin singlet and the odd parity states correspond to pseu-

dospin triplet states. These pseudospin superconducting states lead to important differences from their original spin counterparts which are apparent, for example, when considering a junction between two such materials with different SOC strengths[166].

From the phenomenological GL theory of superconductivity[6,175], we know that the superconducting order parameter has the same symmetry as a Cooper pair wave function. Thus, the antisymmetry of fermionic wave function requires

$$\hat{\Delta}(\boldsymbol{k}) = -\hat{\Delta}^T(-\boldsymbol{k}). \tag{11}$$

Below T_c, it must have the full symmetry of the normal state and can be written in terms of the irreps of G as shown in Eqn. (9). For uniform superconducting instabilities and without any SOC, the structures of the order parameters are determined by the irreps of $G' = G_0 \otimes SO(3)$. If $\hat{\Gamma}^c$ and $\hat{\Gamma}^s$ are the irreps of G_0 and $SO(3)$ respectively, the irreps of G' have the form

$$\hat{\Gamma} = \hat{\Gamma}^c \otimes \hat{\Gamma}^s. \tag{12}$$

Then if $\{\Gamma^c_m(\boldsymbol{k}) : m = 1, \ldots, n_c\}$ forms a basis for $\hat{\Gamma}^c$ with n_c being its dimensionality and $\{\Gamma^s_n : n = 1, \ldots, n_s\}$ forms a basis for $\hat{\Gamma}^s$ with n_s being its dimensionality, we can construct a basis for $\hat{\Gamma}$ as $\Gamma_{m,n}(\boldsymbol{k}) = \Gamma^c_m(\boldsymbol{k})\Gamma^s_n$. The dimensionality of $\hat{\Gamma}$ is then given by $d = n_c n_s$. In the superconducting state, we can write the gap function from Eqn. (9) as

$$\hat{\Delta}(\boldsymbol{k}) = \sum_{m=1}^{n_c}\sum_{n=1}^{n_s} \eta_{m,n}\Gamma^c_m(\boldsymbol{k})\Gamma^s_n. \tag{13}$$

Thus, the order parameters in the singlet representations have the form

$$\hat{\Delta}_{\text{singlet}}(\boldsymbol{k}) = \sum_{m=1}^{n_c} \eta^s_m \Gamma^c_m(\boldsymbol{k})\Gamma^s_{\text{singlet}} = \Gamma^s_{\text{singlet}}\Delta_s(\boldsymbol{k}) \tag{14}$$

requiring (by Eqn. (11)) $\Gamma^s_{\text{singlet}} = -\left(\Gamma^s_{\text{singlet}}\right)^T$ and $\Gamma^c_m(-\boldsymbol{k}) = \Gamma^c_m(\boldsymbol{k})$ which in turn implies $\Delta_s(-\boldsymbol{k}) = \Delta_s(\boldsymbol{k})$, i.e. an even scalar function. The singlet case is thus called an even parity superconducting state. Similarly, in the triplet case, the order parameter can be written as

$$\hat{\Delta}_{\text{triplet}}(\boldsymbol{k}) = \sum_{m=1}^{n_c}\sum_{n=-1,0,1} \eta^t_{m,n}\Gamma^c_m(\boldsymbol{k})\Gamma^s_{triplet,n} \tag{15}$$

requiring (by Eqn. (11)) $\Gamma^s_{triplet,n} = \left(\Gamma^s_{triplet,n}\right)^T$ and $\Gamma^c_m(-\boldsymbol{k}) = -\Gamma^c_m(\boldsymbol{k})$. The triplet case is thus called an odd parity superconducting state.

The spin dependence of the gap function can be compactly written using a general 2×2 matrix formalism as

$$\hat{\Delta}(\boldsymbol{k}) = \begin{bmatrix} \Delta_{\uparrow\uparrow} & \Delta_{\uparrow\downarrow} \\ \Delta_{\downarrow\uparrow} & \Delta_{\downarrow\downarrow} \end{bmatrix}. \tag{16}$$

Then, $\hat{\Delta}(\boldsymbol{k})$ is called the gap matrix. Then the gap matrix for the singlet case is

$$\hat{\Delta}_{\text{singlet}}(\boldsymbol{k}) = \Delta_s(\boldsymbol{k})i\sigma_y = \begin{pmatrix} 0 & \Delta_s(\boldsymbol{k}) \\ -\Delta_s(\boldsymbol{k}) & 0 \end{pmatrix} \tag{17}$$

where $\Delta_s(\boldsymbol{k}) = \Delta_s(-\boldsymbol{k})$ is an even function of $\boldsymbol{k}$. The gap matrix for the triplet case can be written as

$$\begin{aligned}\hat{\Delta}_{\text{triplet}}(\boldsymbol{k}) &= \begin{bmatrix} \Delta_{\uparrow\uparrow} & \Delta_0 \\ \Delta_0 & \Delta_{\downarrow\downarrow} \end{bmatrix} = \begin{bmatrix} -d_x + id_y & d_z \\ d_z & d_x + id_y \end{bmatrix} \\ &= (\boldsymbol{d}(\boldsymbol{k}) \cdot \hat{\boldsymbol{\sigma}})i\sigma_y. \end{aligned} \tag{18}$$

Here, $\hat{\boldsymbol{\sigma}}$ is a vector with the three Pauli spin matrices as its components and $\boldsymbol{d}(\boldsymbol{k}) = -\boldsymbol{d}(-\boldsymbol{k})$ is a complex odd vector function which transforms as a 3D vector under rotation in the spin space.

The $\boldsymbol{d}(\boldsymbol{k})$-vector compactly describes the spin and angular momentum of the Cooper pairs and the nodal structure of the energy gap. In this case, it is instructive to define the vector

$$\boldsymbol{q}(\boldsymbol{k}) = i(\boldsymbol{d}(\boldsymbol{k}) \times \boldsymbol{d}^*(\boldsymbol{k})). \tag{19}$$

Note that $\boldsymbol{q}(\boldsymbol{k})$ is a real even vector function of $\boldsymbol{k}$. Then depending on the value of $\boldsymbol{q}(\boldsymbol{k})$, there are two types of possible triplet pairing: $\boldsymbol{q}(\boldsymbol{k}) = 0$ is called a unitary triplet pairing state and $\boldsymbol{q}(\boldsymbol{k}) \neq 0$ is called a nonunitary triplet pairing state. The finite $\boldsymbol{q}(\boldsymbol{k})$ corresponding to the non-unitary triplet pairing case is of special interest since it implies structural difference in pairing of up spins and down spins along different $\boldsymbol{k}$-directions which in turn results in TRS breaking. In general, we have

$$\hat{\Delta}_{\text{triplet}}(\boldsymbol{k})\hat{\Delta}^\dagger_{\text{triplet}}(\boldsymbol{k}) = |\boldsymbol{d}(\boldsymbol{k})|^2 1_2 + \boldsymbol{q}(\boldsymbol{k}) \cdot \hat{\boldsymbol{\sigma}}. \tag{20}$$

This product plays an important role in distinguishing between the unitary and nonunitary types of pairing states.

For centrosymmetric SCs with strong SOC, the pseudospin singlet and pseudospin triplet order parameters have the same form as in Eqn. (17) and Eqn. (18) respectively. Whereas for noncentrosymmetric SCs with strong SOC, the superconducting state with mixed singlet and triplet components has the gap matrix

$$\hat{\Delta}(\boldsymbol{k}) = [\Delta_s(\boldsymbol{k}) + \boldsymbol{d}(\boldsymbol{k}) \cdot \hat{\boldsymbol{\sigma}}]i\sigma_y. \tag{21}$$

We note that, in general, the singlet gap function $\Delta_s(\boldsymbol{k})$ can be written as

$$\Delta_s(\boldsymbol{k}) = \sum_m c_m \mathcal{Y}_{l,m}(\hat{\boldsymbol{k}}) \text{ with } l = \text{even} \tag{22}$$

and the triplet $\boldsymbol{d}$-vector can be written as

$$\boldsymbol{d}(\boldsymbol{k}) = \sum_{m,n=x,y,z} b_{m,n}\mathcal{Y}_{l,m}(\hat{\boldsymbol{k}})\hat{n} \text{ with } l = \text{odd}. \tag{23}$$

Here, $\mathcal{Y}_{l,m}(\hat{\boldsymbol{k}})$ are the spherical harmonics in the $\boldsymbol{k}$-space, c_m and $b_{m,n}$ are complex coefficients. Thus, these gap

functions are given a nomenclature according to their respective angular momentum quantum number. In general, if the gap matrix satisfies $\hat{\Delta}(\delta \boldsymbol{k}) = \delta^l \hat{\Delta}(\boldsymbol{k})$ for a real number δ, then $l = 0, 1, 2, \ldots$ are called s-wave, p-wave, d-wave, ... superconducting states respectively.

V. TIME REVERSAL SYMMETRY BREAKING ORDER PARAMETERS

We now specialize to the case of SCs which spontaneously break TRS. In what follows, we only consider the types of superconducting states which by themselves break TRS spontaneously at T_c. We do not consider the cases[9] where the superconducting order competes with some form of magnetic order and the superconducting state can coexist with the magnetic order breaking TRS. We also do not consider the possible TRS breaking superconducting ground states such as $s+is'$ or $s+id'$ resulting from competition between superconducting instabilities with different symmetries which would not, by themselves, break TRS. Such superconducting states with a frustrated phase of the order parameter in general require two superconducting transitions and only below the lower transition temperature the superconducting state breaks TRS spontaneously. In general, the two transition temperatures are different and require fine tuning for them to coincide.

We first note that TRS breaking in the superconducting ground state requires a degenerate instability channel corresponding to a multi-dimensional irrep of $\mathcal{G}$. This argument hinges on the fact that a TRS breaking state with order parameter $\hat{\Delta}(\boldsymbol{k})$ under the TRS operation should transform to a new state with order parameter $\hat{\Delta}'(\boldsymbol{k}) = \mathcal{T}\hat{\Delta}(\boldsymbol{k})$ where $\hat{\Delta}'(\boldsymbol{k})$ is not simply related by an overall phase to $\hat{\Delta}(\boldsymbol{k})$. The simplest possible way it can happen is by a multi-component order parameter with nontrivial phase difference between its components. The origin of the multi-component order parameter from a multidimensional irrep of $\mathcal{G}$ can however be very different, for example, it can correspond to the underlying point group G_0 (an example of this is the chiral p-wave state proposed for Sr_2RuO_4[7]), the group of spin rotations $SO(3)$ (for example a nonunitary triplet state with equal spin pairing proposed for the cases of $LaNiC_2$ and $LaNiGa_2$[11–14]) or the TRS group itself (for example the special case of the chiral point group $\mathcal{C}_4$ allowing for a loop-super current ground state[10]).

We note that the classification scheme of the superconducting order parameters discussed in the previous section can lead to many symmetry-allowed TRS breaking channels with similar predicted thermodynamic consequences[165]. Thus, in general it can be very hard to pin down the exact symmetry of the superconducting order parameter by routine probes of unconventional SCs in a real material.

TABLE III. Important basis functions of D_{4h} for the 2 two dimensional irreps corresponding to strong SOC. A_1, A_2 and B_2 are constants independent of $\boldsymbol{k}$.

D_{4h}	Basis functions	
Irreps	Scalar (even)	Vector (odd)
E_g	$A_1 k_z \begin{pmatrix} k_x \\ k_y \end{pmatrix}$	–
E_u	–	$\begin{pmatrix} A_2 k_z \hat{x} + B_2 k_x \hat{z} \\ A_2 k_z \hat{y} + B_2 k_y \hat{z} \end{pmatrix}$

A. Example of a TRS breaking state: a chiral superconductor

We now illustrate how to use the GL formalism outlined above to deduce the possible TRS breaking states of a SC through a particular example.

Chiral SCs[176] are defined as SCs for which the phase of the order parameter winds in a certain direction (clockwise or anticlockwise) while moving in the $\boldsymbol{k}$-space about some axis on the Fermi surface of the underlying metal. The case of a TRS breaking state resulting from a multi-dimensional irrep of the point group is thus very interesting, since it necessarily gives rise to a type of superconducting ground state which is chiral in nature. Also, in this case, since the superconducting ground state breaks additional crystal symmetries, it in general needs an unconventional pairing mechanism (not electron-phonon).

We will now discuss the specific example of constructing TRS breaking superconducting channels in a tetragonal system with the point group symmetry D_{4h}. We will consider the simplest case of symmorphic space group and strong SOC in the following example which is probably relevant for the case of Sr_2RuO_4[7]. The D_{4h} point group has 8 one dimensional irreps (4 of them have even parity and the other 4 have odd parity) and 2 two dimensional irreps (one with even parity denoted by E_g and the other with odd parity denoted by E_u). Centrosymmetry implies that the possible superconducting states are either purely triplet or purely singlet states. Furthermore, a TRS breaking superconducting order parameter is thus possible only in the E_g or the E_u irrep. We will now focus only on these two irreps and construct the possible TRS breaking superconducting order parameters for the system.

We consider strong SOC and then the possible even scalar and odd vector basis functions for the E_g and E_u irreps are listed in Table III. The fourth order invariant corresponding to the 2 two dimensional irreps of D_{4h} gives the quartic order term of the GL free energy[165,166] to be

$$f_4 = \beta_1(|\eta_1|^2 + |\eta_2|^2)^2 + \beta_2|\eta_1^2 + \eta_2^2|^2 + \beta_3(|\eta_1|^4 + |\eta_2|^4) \tag{24}$$

where (η_1, η_2) are the two complex components of the two dimensional order parameters. This free energy now needs to be minimized with respect to both η_1 and η_2. To this end, we write $\eta_j = |\eta_j| e^{i\alpha_j}$ where $|\eta_j|$ is the real

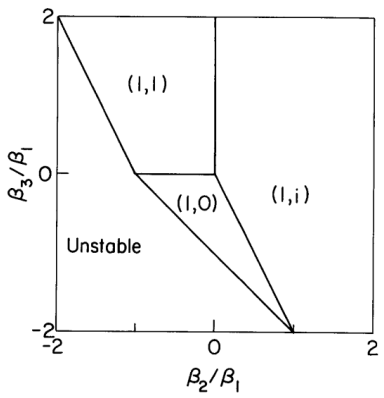

FIG. 8. (Color online) The phase diagram corresponding to the two dimensional irreps of D_{4h}. Reproduced with permission from Ref. 165. Copyright 1990 by Taylor & Francis Ltd.

amplitude and α_j is the phase ($j = 1$ and 2). Then we define $|\eta_1| = |\eta|\cos(\theta)$, $|\eta_2| = |\eta|\sin(\theta)$ and $\alpha = (\alpha_1 - \alpha_2)$. Thus θ determines the relative amplitude and α determines the relative phase of the two components and we take $0 \leq \theta \leq \pi/2$ and $0 \leq \alpha \leq 2\pi$. Then we have

$$(\eta_1, \eta_2) = |\eta| e^{i\alpha_1}[\cos(\theta), \sin(\theta)e^{i\alpha}]. \tag{25}$$

Thus effectively we need to minimize the free energy with respect to the two real variables θ and α. Using the above equation in Eqn. (24), the free energy simplifies to

$$f_4 = |\eta|^4 \left[(\beta_1 + \beta_2 + \beta_3) - \frac{1}{2}\sin^2(2\theta)\{\beta_3 - 2\beta_2 \sin^2(\alpha)\}\right]. \tag{26}$$

To minimize the above free energy with respect to θ and α, we compute and equate the corresponding first derivatives to zero which gives

$$\begin{aligned} \frac{\partial f_4}{\partial \theta} &= 0 \\ \Rightarrow \sin(4\theta)\{\beta_3 - 2\beta_2 \sin^2(\alpha)\} &= 0 \end{aligned} \tag{27}$$

and

$$\begin{aligned} \frac{\partial f_4}{\partial \alpha} &= 0 \\ \Rightarrow \beta_2 \sin^2(2\theta)\sin(2\alpha)\} &= 0 \end{aligned} \tag{28}$$

assuming $|\eta| \neq 0$. The above two equations give the following nontrivial and inequivalent solutions: $(\eta_1, \eta_2) = (1, 0)$, $\frac{1}{\sqrt{2}}(1, 1)$ and $\frac{1}{\sqrt{2}}(1, i)$. The corresponding phase diagram is shown in Fig. 8 (reproduced from Ref. 165). We note that there is an extended region in the parameter space where the states corresponding to $(\eta_1, \eta_2) = \frac{1}{\sqrt{2}}(1, i)$ is stabilized. The instabilities corresponding to this case spontaneously break TRS at T_c due to a nontrivial phase difference between the two order parameter components. The even parity TRS breaking superconducting order parameter belonging to E_g is given by

$$\Delta(\boldsymbol{k}) = \Delta_0 k_z(k_x + ik_y) \tag{29}$$

where Δ_0 is the real amplitude independent of $\boldsymbol{k}$. This is a *chiral d-wave* singlet order parameter. The odd parity superconducting order parameter belonging to E_u gives rise to the TRS breaking triplet state with the d-vector given by

$$\boldsymbol{d}(\boldsymbol{k}) = [Ak_z, iAk_z, B(k_x + ik_y)]\,. \tag{30}$$

Here, A and B are material dependent real constants independent of $\boldsymbol{k}$ and in general they are nonzero. We note that the values of A and B determine the orientation of the d-vector. For example, for $A = 0$ the d-vector points along the c-axis and for $B = 0$ the d-vector points in the ab-plane. We also note that

$$\boldsymbol{d}(\boldsymbol{k}) \times \boldsymbol{d}^*(\boldsymbol{k}) = 2iAk_z(Bk_x\hat{x} - Bk_y\hat{y} - Ak_z\hat{z}) \tag{31}$$

which is nonzero in general. Hence, this superconducting state is a *nonunitary chiral p-wave* triplet state. The special case of $A = 0$ is the unitary chiral p-wave triplet case, which was previously applied to the case of Sr_2RuO_4 (see Sec. III A for an overview of recent developments).

B. Topological properties

Topology is a concept in mathematics dealing with properties of geometric objects preserved under continuous deformations of their shapes. In quantum mechanics, the wave function defined on a certain parameter space can have a "twist" and thus may not be adiabatically connected to itself for different parameter values. Then the wave function is said to be topologically non-trivial. In condensed phases, when a quantum many-body wave function is adiabatically connected to its atomic limit, it is topologically trivial[178]. The topology of a system is typically characterized by integer topological invariants which can be used for topological classification. The first example of a topological condensed matter system[179] is the quantum Hall state and the topological invariant in this case is the Chern number.

The basic ingredient for the topological classification of quantum many body systems is a gap in the energy spectrum protecting the occupied states. The superconducting state within the Bogoliubov-de Gennes (BdG) mean-field theory, described in Section VI, has all the negative energy quasi-particle states fully occupied and these are usually protected by a gap. Hence, depending on the symmetries and dimensionality both insulators and fully gapped superconductors are classified in a similar way by the "ten-fold" classification scheme[180]. They are characterized by their global bulk topological invariants. In general, when a superconductor possesses a non zero bulk topological invariant it is called a topological superconductor.

The bulk topological invariants can be defined in general by using the occupied Bloch wave functions of electrons or quasiparticles. The momentum-dependent occupied Bloch states can be thought of as a mapping of the

first Brillouin zone onto the Hilbert space and the image can have "winding" depending on the type of wave functions such that it cannot be deformed smoothly to a point. In an abstract sense then the topological invariant is the *winding number* of the image of the first Brillouin zone on the Hilbert space[179]. Thus the topological invariant can have only integer values and as long as there is no singularity it cannot change discontinuously. Such a singularity arises when the bulk gap closes and the definition of the topological invariant based on occupied states is no longer valid. As a result the topological invariant can change discontinuously in this case. When we consider an interface between a topological system and a topologically trivial state such as vacuum, the topological invariant changes discontinuously at the interface requiring the bulk gap to close. As a result there are topologically protected gapless interface states. This is called the *bulk-boundary correspondence*[179,180].

Topological superconductors[178,181] are usually rare and often require unconventional pairing symmetries. Unconventional superconductors on the other hand often feature nodes in their excitation spectrum. As a result they are *prima facie* not covered by the tenfold classification scheme and global topological invariants are not defined for them. However, if we consider momenta in certain directions as parameters of the system then for fixed values of these momenta a nodal superconductor can be effectively thought as a fully gapped system with reduced dimensionality. Then momentum-dependent topological invariants can be defined. As a result, from the bulk-boundary correspondence nodal topological superconductors also possess topologically protected gapless surface states although their topological protection is weaker than that found for fully-gapped topological superconductors[178,179,181]. Moreover superconductors where nodes are accidental, i.e. not required by symmetry, can feature topologically-distinct fully-gapped phases in their phase diagrams, separated by gapless phases where the topology can re-arrange itself[182–184]. The phase transitions involved in going from one fully-gapped phase to another in this case have distinct thermodynamic signatures[184,185].

The most prominent feature of topological superconductors is that their gapless surface excitations are Majorana fermions. A Majorana fermion is a neutral particle which is its own anti-particle and obeys the Dirac equation. Since excitations in a superconductor are particle-hole excitations, the zero-energy excitations are naturally their own anti-particles and the Hamiltonian describing the low-energy physics has a linear dispersion obeying the Dirac equation. The Majorana excitations found at the boundaries, such as physical interfaces or inside vortices, are the zero-energy Andreev bound states[178,179]. These zero-energy bound states give rise to mid-gap states strongly affecting the transport properties of a topological superconductor. They give rise to zero-bias conductance peaks visible in the tunnelling experiments for example. Topologically protected Majorana fermions inside the vortices of topological superconductors have non-Abelian statistics and are promising candidates for topological quantum computation[186].

While many topological states are protected by TRS, and therefore cannot be realised in a TRS-breaking superconducting state, this is not always the case. One example of TRS breaking topological superconducting state is the chiral $(p_x + ip_y)$ state believed to be realized in the A-phase of He^3[178,179,181]. The pairing potential for the state is given by $\Delta(\boldsymbol{k}) = \frac{\Delta_0}{k_F}(k_x \pm ik_y)$ where k_F is the Fermi wave vector and Δ_0 is a real constant. Considering a single band normal state with a spherical Fermi surface, the BdG Hamiltonian for the $p_x - ip_y$ state can be written as

$$H(\boldsymbol{k}) = \mathbf{N}(\boldsymbol{k}) \cdot \boldsymbol{\sigma} \tag{32}$$

where $\boldsymbol{\sigma}$ is the vector of the three Pauli matrices and $\mathbf{N}(\boldsymbol{k}) = \left(\frac{\Delta_0}{k_F}k_x, \frac{\Delta_0}{k_F}k_y, h(\boldsymbol{k})\right)$ is a Pseudospin vector. The normal state dispersion is $h(\boldsymbol{k}) = \frac{\hbar^2}{2m}\left(k^2 - k_F^2\right)$. The eigenvalues of the Hamiltonian in Eqn. (32) are $\pm E(\boldsymbol{k})$ where

$$E(\boldsymbol{k}) = |\mathbf{N}(\boldsymbol{k})| = \sqrt{h^2(\boldsymbol{k}) + \frac{\Delta_0^2}{k_F^2}\left(k_x^2 + k_y^2\right)}. \tag{33}$$

Hence, the superconducting ground state has two point nodes at the two poles of the Fermi surface $(0, 0, \pm k_F)$ which are also Weyl nodes. The corresponding Bloch wave functions $|u_\pm(\boldsymbol{k})\rangle$ are eigenfunctions of $\hat{\mathbf{n}}(\boldsymbol{k}).\boldsymbol{\sigma}$ with eigenvalues ± 1 where $\hat{\mathbf{n}}(\boldsymbol{k}) = \mathbf{N}(\boldsymbol{k})/|\mathbf{N}(\boldsymbol{k})|$ is the unit vector along the direction of the pseudospin. In spherical coordinates, parametrizing $\hat{\mathbf{n}}(\boldsymbol{k}) = [n_x(\boldsymbol{k}), n_y(\boldsymbol{k}), n_z(\boldsymbol{k})] = [\sin(\theta)\cos(\phi), \sin(\theta)\sin(\phi), \cos(\theta)]$ we have

$$|u_-(\boldsymbol{k})\rangle = \begin{bmatrix}\cos(\frac{\theta}{2})e^{-i\phi}\\ \sin(\frac{\theta}{2})\end{bmatrix} \text{ and } |u_+(\boldsymbol{k})\rangle = \begin{bmatrix}\sin(\frac{\theta}{2})e^{-i\phi}\\ -\cos(\frac{\theta}{2})\end{bmatrix} \tag{34}$$

Then from the negative energy occupied states $|u_-(\boldsymbol{k})\rangle$ the Berry connection is defined as

$$\mathbf{A}(\boldsymbol{k}) = i\langle u_-(\boldsymbol{k})|\boldsymbol{\nabla}_{\boldsymbol{k}}|u_-(\boldsymbol{k})\rangle \tag{35}$$

and the corresponding Berry curvature is $\mathbf{F}(\boldsymbol{k}) = \boldsymbol{\nabla}_{\boldsymbol{k}} \times \mathbf{A}(\boldsymbol{k})$. In terms of the components of $\hat{\mathbf{n}}(\boldsymbol{k})$, it is given by $\mathbf{F}(\boldsymbol{k}) = [n_y(\boldsymbol{k})\{\boldsymbol{\nabla}_{\boldsymbol{k}} n_z(\boldsymbol{k}) \times \boldsymbol{\nabla}_{\boldsymbol{k}} n_x(\boldsymbol{k})\} - n_x(\boldsymbol{k})\{\boldsymbol{\nabla}_{\boldsymbol{k}} n_z(\boldsymbol{k}) \times \boldsymbol{\nabla}_{\boldsymbol{k}} n_y(\boldsymbol{k})\}]/[2\{n_x^2(\boldsymbol{k}) + n_y^2(\boldsymbol{k})\}]$. For the chiral p-wave case, $F_x(\boldsymbol{k})$ and $F_y(\boldsymbol{k})$ are odd functions of (k_y, k_z) and (k_x, k_z) respectively. Hence, there is no Berry flux along the x and y directions. The number of field lines coming in and out of the ca and cb planes are the same. $F_z(\boldsymbol{k})$ is an even function of (k_x, k_y) and the flux through the ab plane as a function of k_z is

$$\Phi(\boldsymbol{k}) = \int dk_x dk_y F_z(\boldsymbol{k}) = 2\pi\mathcal{C}(k_z). \tag{36}$$

$\mathcal{C}(k_z)$ is the Chern number of the effective 2D problem for a fixed k_z. For a given value of $|k_z| < k_F$, the Hamiltonian in Eqn. (32) describes an effective 2D problem

with fully gapped weak coupling BCS pairing and an effective chemical potential $\frac{\hbar^2}{2m}(k_F^2 - k_z^2)$ having the Chern number $C(k_z) = +1$. For $|k_z| > k_F$, the effective chemical potential is negative and describes a topologically trivial BEC state. The Weyl point nodes at $(0, 0, \pm k_F)$ act as monopoles and anti-monopoles of the Berry curvature and the flux through a sphere surrounding the monopole is 2π and that through the anti-monopole is -2π. The topologically protected Weyl nodes give rise to Majorana arc surface states on the surface Brillouin zone corresponding to the $(1, 0, 0)$ and $(0, 1, 0)$ surfaces having chiral linear dispersions along y and x directions respectively. As a result of the arc surface states the system shows anomalous thermal and spin Hall effects[181]. Other prominent examples of TRS breaking chiral superconductors include the chiral f-wave pairing state[187] with pairing potential $\Delta(\boldsymbol{k}) \propto k_z(k_x + ik_y)^2$ believed to be realized in UPt_3 and the chiral p-wave state proposed for UTe_2[188].

C. Band structure

The normal-state properties of most superconductors are determined by their band structure. For some systems it is possible to obtain this experimentally using techniques such as quantum oscillations[189] (which requires samples with long mean free paths) and ARPES[190] (feasible for layered materials that can be cleaved cleanly). More habitually, the band structure can be calculated from first principles using density functional theory (DFT)[191]. Band structures of many materials whose supercondcuting state breaks TRS have been obtained in this way (sometimes before it was known that they had this property). To cite just a few examples, such information is available in the literature for Sr_2RuO_4[192,193], $LaNiGa_2$[177,194], Re_6Zr[131] and La_7Ir_3[119]. Since the band structure is a property of the normal state, reviewing such work is beyond the scope of the present review. We nevertheless shall point out here several ways in which features of the band structure may have a bearing on the question of broken TRS. We will use the case of $LaNiGa_2$ considered in the Ref. 177 as our chief example, with some other systems mentioned to illustrate specific points as the need arises.

A common feature of most of these materials is that there are multiple bands crossing the Fermi level leading to several Fermi surface sheets. These bands can arise from several orbitals of one or more types of atoms in the several symmetry related sites. The information about the most important orbitals, for example, can be obtained by computing the projected density of states (DOS) of these orbitals and looking at their contribution to the total density of states at the Fermi level. For the case of $LaNiGa_2$, there are several bands crossing the Fermi level and they arise mainly from the p-orbitals of Ga and d-orbitals of Ni. As a result the shape of the Fermi surface sheets are quite complicated in this example. DFT calculations can also be used to obtain the strength of SOC on the Fermi surface[194] which, as we discussed earlier, can have dramatic effects on the pairing symmetry depending on the presence or absence of inversion symmetry in the material.

Beyond the determination of normal-state properties, DFT calculations can be used as a starting point for microscopic theories of the superconducting instability. For instance, in the case of $LaNiGa_2$, assuming phonon-mediated pairing it was shown that a non-relativsitic Eliashberg theory featuring ordinary, singlet s-wave pairing could be used to predict the correct value of T_c[195] - though the one-dimensionality of the irreducible representations of the point group of the crystal makes such theory fundamentally incompatible with broken TRS[12]. One can also take hybrid approaches where DFT is combined with a phenomenological pairing interaction. Such approach has been used recently[15] to show that an internally-antisymmetric, non-unitary tiplet (INT) pairing interaction can describe the experimental data of $LaNiGa_2$ quantitatively with a single adjustable parameter, fixed by the critical temperature T_c.

More flexible models can be obtained by fitting the band structure near the Fermi level to a tight-binding Hamiltonian including the "few" most important orbitals of the material. Then for a "manageable" size of the Hamiltonian one can make sure that the normal state band structure near the Fermi level, the topology of the Fermi surfaces and the density of states near the Fermi level is faithfully represented by this normal state Hamiltonian. This normal state Hamiltonian can then be used in conjunction with the pairing models deduced from symmetry to predict and compare experimentally observable quantities.

Finally, the topology of the Fermi surfaces plays an important role in determining the thermodynamic properties of the TRS breaking superconducting ground states. For example, even if an order parameter features nodes at certain regions of the Brillouin zone, if the Fermi surfaces are open or have necks in that region, the thermodynamic features of the system will behave similar to that of a fully gapped state. For instance, the three Fermi surfaces of Sr_2RuO_4 are quasi-two dimensional and open along the k_z direction, which would make the poles of the chiral state at $k_x = k_y = 0$ compatible with fully-gapped behaviour[7].

D. Estimation of internal magnetic field/magnetic moment

Estimating the strength of the internal magnetic field or the magnetic moment is in general a nontrivial task. This is because of the following reasons.

1. Firstly, the magnetic moment per unit cell of the superconducting state μ_s depends on the details of the pairing model. For example, for a chiral SC such as one with the chiral p-wave triplet state, the

magnetic moment can be estimated from the corresponding orbital angular momentum[196,197]. For a material with the loop-super current ground state[10] proposed to be realized in Re_6(Zr, Hf, Ti), the spontaneous internal magnetic field can be estimated from the super-current in the ground state. For $LaNiGa_2$, from a semi-first principles approach we can directly compute the spontaneous magnetic moment due to the non-unitary triplet state[15].

2. Secondly, even if the magnetic moment μ_s can be accurately predicted, the muon does not measure μ_s but the induced internal field $\mathbf{B}_{\rm int}(\mathbf{r})$ which depends, on an atomic scale, on the location $\mathbf{r}$ of the muon within the unit cell– an averaged magnetic moment is therefore not enough to make a quantitative prediction.

3. Thirdly, given that the muon is a strong local perturbation, an understanding of the way the muon changes the local crystal and electronic structure of the sample is essential for a quantitative prediction.

While a naive estimate of the internal field $B_{\rm int} \sim \mu_0\mu_s/4\pi abc$ gives the right order of magnitude for Re_6Zr[10] and $LaNiGa_2$[15] overcoming the issues in points 2 and 3, above, is essential in order to develop a quantitative understanding of zero-field μSR in SCs with broken TRS. Indeed, in SCs any intrinsic fields ought to be, in the bulk, fully screened by the Meissner field, so the only reasonable interpretation of the ability of the muon to detect the intrinsic field is that the muon itself locally suppresses the order parameter. In this picture, what the muon sees in fact is the screening field, rather than the intrinsic magnetisation[198]. Ref.[196] contains the only quantitative calculation realizing this scenario, in a very simplified model of a chiral SC. Meanwhile current DFT studies of the effect of the muon on the local crystal and electronic structure[199,200] have not yet been extended to SCs.

VI. MEAN FIELD THEORY

In this section we review the generalized BCS/Bogoliubov-de Gennes theory[166], which is an essential tool for computing the excitation spectra and predicting experimental observables for a particular superconducting ground state.

A. General formalism

A general Hamiltonian describing pairing of electrons in momentum space can be written as

$$\mathcal{H} = \sum_{\boldsymbol{k},\sigma} \xi(\boldsymbol{k}) c^\dagger_{\boldsymbol{k},\sigma} c_{\boldsymbol{k},\sigma} + \frac{1}{2} \sum_{\boldsymbol{k},\boldsymbol{k}',\bar{\boldsymbol{q}},\{\sigma_i\}} V_{\{\sigma_i\}}(\boldsymbol{k},\boldsymbol{k}') c^\dagger_{\frac{\bar{\boldsymbol{q}}}{2}+\boldsymbol{k},\sigma_1} c^\dagger_{\frac{\bar{\boldsymbol{q}}}{2}-\boldsymbol{k},\sigma_2} c_{\frac{\bar{\boldsymbol{q}}}{2}-\boldsymbol{k}',\sigma_3} c_{\frac{\bar{\boldsymbol{q}}}{2}+\boldsymbol{k}',\sigma_4} \tag{37}$$

where $c^\dagger_{\boldsymbol{k},\sigma}$ creates an electron with momentum $\boldsymbol{k}$ and spin σ and $\xi(\boldsymbol{k}) = (\epsilon(k) - \mu)$ with μ being the chemical potential and $\epsilon(\boldsymbol{k})$ being the normal state dispersion. $V_{\sigma_1,\sigma_2,\sigma_3,\sigma_4}(\boldsymbol{k},\boldsymbol{k}')$ describes the elements of the pairing interaction $\hat{V}$ between two electrons and includes the possibility of formation of pairs with finite total momentum $\bar{\boldsymbol{q}}$. We will, however, consider only the case of zero total momentum ($\bar{\boldsymbol{q}} = 0$) pairs with the only nonzero matrix elements

$$V_{\sigma_1,\sigma_2,\sigma_3,\sigma_4}(\boldsymbol{k},\boldsymbol{k}') = \left\langle \boldsymbol{k},\sigma_1;-\boldsymbol{k},\sigma_2|\hat{V}|-\boldsymbol{k}',\sigma_3;\boldsymbol{k}',\sigma_4 \right\rangle. \tag{38}$$

The pairing interaction $\hat{V}$ can have different origins including being mediated by phonons[201] or spin-fluctuations[202] for example. The important point to note is that the interaction is attractive within a narrow window near the Fermi level and the Fermi surface is unstable to this attractive interaction leading to the formation of Cooper pairs. To find the ground state properties of the system, we decompose the quartic interaction term by introducing mean-fields using a standard Curie-Weiss type mean-field theory[201] and ignoring fluctuations above the mean-field ground state —although fluctuations above the mean-field ground state can be systematically taken into account when necessary[175]. We define the mean-field pairing potential or the gap function as

$$\Delta_{\sigma,\sigma'}(\boldsymbol{k}) = \sum_{\boldsymbol{k}',\sigma_1,\sigma_2} V_{\sigma,\sigma',\sigma_1,\sigma_2}(\boldsymbol{k},\boldsymbol{k}') \langle c_{-\boldsymbol{k}',\sigma_1} c_{\boldsymbol{k}',\sigma_2} \rangle \tag{39}$$

with $\Delta_{\sigma,\sigma'}(\boldsymbol{k})$ being the elements of the gap matrix $\hat{\Delta}(\boldsymbol{k})$ satisfying Eqn. (11). Introducing these mean-fields, the Hamiltonian within the mean-field approximation takes the form

$$\mathcal{H}_{MF} = \sum_{\boldsymbol{k},\sigma} \xi(\boldsymbol{k}) c^\dagger_{\boldsymbol{k},\sigma} c_{\boldsymbol{k},\sigma} + \frac{1}{2} \sum_{\boldsymbol{k},\sigma,\sigma'} [\Delta_{\sigma,\sigma'}(\boldsymbol{k}) c^\dagger_{\boldsymbol{k},\sigma} c^\dagger_{-\boldsymbol{k},\sigma'} + h.c.]. \tag{40}$$

We now use the BdG formalism to find the ground state of this mean-field Hamiltonian. To this end, we define the Nambu spinor as

$$\Psi_{\boldsymbol{k}} = \begin{pmatrix} \hat{c}_{\boldsymbol{k}} \\ \hat{c}^{\dagger T}_{-\boldsymbol{k}} \end{pmatrix} \quad \text{with } \hat{c}_{\boldsymbol{k}} = \begin{pmatrix} c_{\boldsymbol{k}\uparrow} \\ c_{\boldsymbol{k}\downarrow} \end{pmatrix}. \tag{41}$$

Then the mean-field Hamiltonian takes the form

$$\mathcal{H}_{MF} = \frac{1}{2} \sum_{\boldsymbol{k}} \Psi^\dagger_{\boldsymbol{k}} \mathcal{H}_{BdG}(\boldsymbol{k}) \Psi_{\boldsymbol{k}} + E'_g \tag{42}$$

where $E'_g = \sum_{\boldsymbol{k}} \xi(\boldsymbol{k})$ gives a constant shift of the ground state energy and will be ignored from here on. Defining $\hat{\xi}_{\boldsymbol{k}} = \xi(\boldsymbol{k})\mathcal{I}_2$ with $\mathcal{I}_n$ being the identity matrix of order n, the BdG Hamiltonian can be written as

$$\mathcal{H}_{BdG}(\boldsymbol{k}) = \begin{pmatrix} \hat{\xi}_{\boldsymbol{k}} & \hat{\Delta}(\boldsymbol{k}) \\ \hat{\Delta}^\dagger(\boldsymbol{k}) & -\hat{\xi}_{\boldsymbol{k}} \end{pmatrix}. \tag{43}$$

This Hamiltonian can be diagonalized using a unitary transformation defined as

$$\hat{U}^\dagger_{\boldsymbol{k}} \mathcal{H}_{BdG}(\boldsymbol{k}) \hat{U}_{\boldsymbol{k}} = \hat{\mathcal{E}}_{\boldsymbol{k}} \; ; \; \hat{U}^\dagger_{\boldsymbol{k}} \hat{U}_{\boldsymbol{k}} = \hat{U}_{\boldsymbol{k}} \hat{U}^\dagger_{\boldsymbol{k}} = \mathcal{I}_4 \tag{44}$$

$$\text{with } \hat{\mathcal{E}}_{\boldsymbol{k}} = \begin{pmatrix} E_{\boldsymbol{k},1} & 0 & 0 & 0 \\ 0 & E_{\boldsymbol{k},2} & 0 & 0 \\ 0 & 0 & -E_{\boldsymbol{k},1} & 0 \\ 0 & 0 & 0 & -E_{\boldsymbol{k},2} \end{pmatrix}. \tag{45}$$

$E_{\boldsymbol{k},\alpha}$ are dispersions of the two branches of the Bogoliubov quasiparticles labeled by $\alpha = 1$ and 2 given by

$$E_{\boldsymbol{k},\alpha} = \sqrt{\xi^2(\boldsymbol{k}) + \frac{1}{2} Tr[\Delta(\boldsymbol{k})\Delta^\dagger(\boldsymbol{k})] + (-1)^\alpha |\boldsymbol{q}(\boldsymbol{k})|}. \tag{46}$$

The mean-field Hamiltonian in Eqn. (42) can then be written as

$$\mathcal{H}_{MF} = \frac{1}{2} \sum_{\boldsymbol{k}} \Gamma^\dagger_{\boldsymbol{k}} \hat{\mathcal{E}}_{\boldsymbol{k}} \Gamma_{\boldsymbol{k}} = \sum_{\boldsymbol{k},\alpha} E_{\boldsymbol{k},\alpha} \gamma^\dagger_{\boldsymbol{k},\alpha} \gamma_{\boldsymbol{k},\alpha} + E''_g \tag{47}$$

where we have defined the creation operator of the Bogoliubov quasiparticles with momentum $\boldsymbol{k}$ in branch α as $\gamma^\dagger_{\boldsymbol{k},\alpha}$ and

$$\Gamma_{\boldsymbol{k}} = \hat{U}^\dagger_{\boldsymbol{k}} \Psi_{\boldsymbol{k}} = \begin{pmatrix} \hat{\gamma}_{\boldsymbol{k}} \\ \hat{\gamma}^{\dagger T}_{-\boldsymbol{k}} \end{pmatrix} \text{ with } \hat{\gamma}_{\boldsymbol{k}} = \begin{pmatrix} \gamma_{\boldsymbol{k},1} \\ \gamma_{\boldsymbol{k},2} \end{pmatrix}. \tag{48}$$

$E''_g = \frac{1}{2}\sum_{\boldsymbol{k},\alpha} E_{\boldsymbol{k},\alpha}$ also gives a constant shift in the ground state energy and will be ignored in the following discussion. The Bogoliubov quasiparticle operators obey fermionic anti-commutation relations

$$\left\{ \gamma^\dagger_{\boldsymbol{k}_1,\alpha_1}, \gamma_{\boldsymbol{k}_2,\alpha_2} \right\} = \delta_{\boldsymbol{k}_1,\boldsymbol{k}_2} \delta_{\alpha_1,\alpha_2}. \tag{49}$$

We note from Eqn. (47) that the mean-field ground state is a free Fermi gas of Bogoliubov quasiparticles and we can define the thermal averages in this ground state as

$$\left\langle \gamma^\dagger_{\boldsymbol{k}_1,\alpha_1} \gamma_{\boldsymbol{k}_2,\alpha_2} \right\rangle = \delta_{\boldsymbol{k}_1,\boldsymbol{k}_2} \delta_{\alpha_1,\alpha_2} f(E_{\boldsymbol{k}_1,\alpha_1}) \tag{50}$$

where $f(x) = (1 + e^{\beta x})^{-1}$ is the Fermi-Dirac distribution function with $\beta = (k_B T)^{-1}$. Taking the form

$$\hat{U}_{\boldsymbol{k}} = \begin{pmatrix} \hat{u}_{\boldsymbol{k}} & \hat{v}_{\boldsymbol{k}} \\ \hat{v}^*_{-\boldsymbol{k}} & \hat{u}^*_{-\boldsymbol{k}} \end{pmatrix}, \tag{51}$$

we can explicitly write the Bogoliubov transformation of the fermion operators as

$$c_{\boldsymbol{k},\sigma} = \sum_{\sigma'} \left[u_{\sigma,\sigma'}(\boldsymbol{k}) \gamma_{\boldsymbol{k},\sigma'} + v_{\sigma,\sigma'}(\boldsymbol{k}) \gamma^\dagger_{-\boldsymbol{k},\sigma'} \right]. \tag{52}$$

This expression of the fermion operators can now be used to find the expectation value of any operator in the mean-field ground state. In particular, Eqn. (39) leads to the self-consistency equation for the gap function and determines the temperature dependence of $\hat{\Delta}(\boldsymbol{k})$ and T_c.

We note from Eqn. (46) that the two branches of the quasiparticle dispersions are degenerate for singlet and unitary-triplet pairings but a non-unitary triplet pairing state lifts this degeneracy leading to two momentum dependent gaps $\sqrt{\frac{1}{2}Tr[\Delta(\boldsymbol{k})\Delta^\dagger(\boldsymbol{k})] \pm |\boldsymbol{q}(\boldsymbol{k})|}$. This splitting is a consequence of reduction in the symmetry in the superconducting state due to broken TRS caused by the non-unitary pairing.

B. Low-temperature thermodynamics characterizing unconventional superconductivity

To determine the behaviors of the experimental observables, such as specific heat (C), penetration depth (λ), NMR relaxation rate ($1/T_1$) and superfluid density (ρ_s), which are routinely measured to characterize unconventional SCs, it is important to consider the behavior of the DOS of the quasiparticle excitations (qpDOS)[166]. Depending on the symmetry of the superconducting order parameter, the low energy behavior of the qpDOS can be qualitatively different and thus leads to characteristic low temperature behaviors of the experimental observables. The qpDOS is defined as

$$g(E) = \sum_{\boldsymbol{k},\alpha} \delta(E - E_{\boldsymbol{k},\alpha}). \tag{53}$$

First, let us discuss the case of conventional rotationally symmetric s-wave SCs. In this case, the system is fully gapped and only with energy above the energy gap excitations are possible. As a result, the qpDOS in this case is given by

$$g(E) = N(0) \frac{E}{\sqrt{E^2 - \Delta(0)^2}} \Theta(E - \Delta(0)) \tag{54}$$

where $N(0)$ is the normal state DOS at the Fermi level and $\Delta(0)$ is the size of the gap at zero temperature. Hence, the qpDOS is zero within the gap and has a coherence peak at $E = \Delta(0)$ visible in single particle tunneling experiments[175] for example. In general, the above type of qpDOS leads to an exponential suppression in the observables at low temperatures.

For an unconventional SCs, however, the presence of nodes in the quasiparticle spectrum leads to a starkly

different qpDOS. The low energy behavior[166,184,185] of the qpDOS for an unconventional SC is

$$g(E) \propto E \quad \text{for line nodes,} \tag{55}$$
$$\propto E^2 \quad \text{for point nodes.} \tag{56}$$

This type of low energy qpDOS in general leads to a power law dependence in the low temperature properties of the observables. The low temperature dependence of the observables under consideration can be computed from the following relations[185] valid for $T \ll T_c$:

$$C(T) \propto \beta \int_0^\infty dE\ g(E)E^2 \left(-\frac{\partial f(E)}{\partial E}\right), \tag{57}$$
$$\Delta\lambda(T) \propto \int_0^\infty dE\ g(E) \left(-\frac{\partial f(E)}{\partial E}\right), \tag{58}$$
$$\frac{1}{T_1T} \propto \int_0^\infty dE\ g^2(E) \left(-\frac{\partial f(E)}{\partial E}\right), \tag{59}$$
$$\left(\frac{\rho_s(T)}{\rho_s(0)} - 1\right) \propto -\Delta\lambda(T) \tag{60}$$

where $\Delta\lambda(T) = [\lambda(T) - \lambda(0)]$. Using the expressions of the qpDOS from Eqn. (55) and Eqn. (56) in the above expressions we can now compute the low temperature behaviors of the observables[166,184,185]:

$$C(T) \propto T^2 \quad \text{for line nodes,} \tag{61}$$
$$\propto T^3 \quad \text{for point nodes.} \tag{62}$$
$$\Delta\lambda(T) \propto T \quad \text{for line nodes,} \tag{63}$$
$$\propto T^2 \quad \text{for point nodes.} \tag{64}$$
$$\frac{1}{T_1T} \propto T^2 \quad \text{for line nodes,} \tag{65}$$
$$\propto T^4 \quad \text{for point nodes.} \tag{66}$$

As noted above the full mean-field description of a given system requires the self-consistent solution of the BdG equations and the mean field self-consistency equations. Nevertheless we note that a lot of information can be obtained by solving the BdG equations for a given form of the pairing potential, obtained by symmetry analysis. Unlike the self-consistency equations, the BdG equations do not feature the pairing interaction. Indeed the results in Eqs. (61)-(66) depend only on the basic features of the pairing potential and Fermi surface topology (shape), and therefore can be used to correlate experimental data with a GL analysis without recourse to a model of the electron-electron pairing interaction. This is an extremely useful weapon in the arsenal of the theorist trying to pry information about the pairing state of a SC out of the available experimental data.

VII. NOVEL GROUND STATES IN MULTIBAND SUPERCONDUCTORS

Superconductivity in systems with multiple bands is usually considered to be effectively occurring in a single band with a gap which has nontrivial momentum dependence in the different Fermi surface sheets of the material as discussed in the previous sections. But recent studies[170,203–209] in many multiband systems such as the iron-based SCs, half-Heusler compounds, UPt_3 and Sr_2RuO_4 have pointed out that internal electronic degrees of freedom, coming from the orbitals or sublattice for example, can give rise to a nontrivial structure to the Cooper pair wave function and in particular to Cooper pairs with higher spins. However, this type of nontrivial superconducting pairing state is usually hard to distinguish from its trivial counterpart since both have qualitatively similar low energy properties.

A. Internally-antisymmetric nonunitary triplet pairing in $LaNiC_2$ and $LaNiGa_2$

We emphasize two cases, $LaNiC_2$ and $LaNiGa_2$, where the group-theoretical analysis seems to be at odds with the experimental results for TRS breaking superconducting order parameters. In both the cases, the symmetry analysis suggests a nodal TRS-breaking nonunitary triplet superconducting state[11–13] while experiments suggest a nodeless, two-gap behavior[14,112].

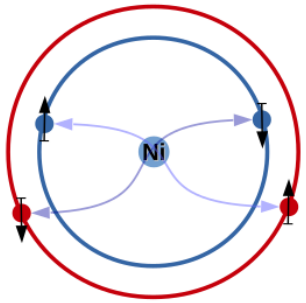

FIG. 9. (Color online) Schematic of a non-unitary triplet pairing between same spins between two different Ni orbitals. Reproduced from Ref. 210, available under a Creative Commons Attribution 4.0 International (CC-BY 4.0) license.

$LaNiC_2$ crystallizes in a noncentrosymmetric orthorhombic crystal structure[11] with symmorphic space group $Amm2$ (No. 38) and point group C_{2v} whereas $LaNiGa_2$ crystallizes in a centrosymmetric orthorhombic crystal structure[13] with symmorphic space group $Cmmm$ (No. 65) and point group D_{2h}. Both the point groups C_{2v} and D_{2h} have only one dimensional irreps. Thus from the point group symmetry alone there is no degenerate instability channel which can potentially lead to a TRS breaking order parameter. Based on this observation, it was proposed[11–14] that considering the effect of SOC to be negligible in both the materials, the three dimensional spin rotation group $SO(3)$ can provide a nonunitary triplet channel which by its very nature breaks TRS spontaneously at T_c. Based on the GL analysis[13] it was shown that a paramagnetic coupling to the magnetisation can stabilize such a nonunitary triplet ground state. This

nonunitary state in turn produces a pseudomagnetic field which splits the up and down spin Fermi surfaces generating an imbalance between the two spin species[13,211]. As a result a subdominant order parameter, induced magnetization, arises and it increases linearly near T_c with decreasing temperature. But the corresponding nonunitary gap functions have nodes. This prompted the suggestion[14] that the pairing state may involve an orbital or band index. Such internal degrees of freedom *cannot* be used to increase the dimensionality of the order parameter i.e. we still need a nonunitary triplet pairing state to break TRS– which in any case is strongly supported by the observation in $LaNiC_2$ of the magnetization signal predicted[13] by the GL theory of the nonunitary state. However, they can dramatically alter the quasiparticle spectrum by ensuring fermionic anti-symmetry without the need for a **k**-dependent gap function, potentially leading to the required **k**-independent gap. The pairing in the superconducting ground state can be between same spins but involving two different orbitals as shown for example with two d-orbitals of the Ni atom in the Fig. 9. Thus the Cooper pair wave function is triplet in the spin sector but has isotropic even parity gap symmetry. Then the two gaps correspond to the two different spin species of different population rather than two different orbital character bands in this internally-antisymmetric nonunitary triplet (INT) ground state. A semi-phenomenological model of $LaNiGa_2$ featuring a detailed, *ab initio* description of the band structure and a *single* adjustable parameter (namely the strength of the effective electron-electron, which is fixed by T_c) in the INT state reproduces the specific heat dependence on temperature very accurately[15] strongly suggesting that this model is an accurate description of the physics of this material.

The mechanism behind such an unusual pairing state remains to be determined, but measurements of $LaNiC_2$ under pressure suggested that the superconductivity is situated on a dome, in close proximity to a correlated phase and quantum criticality[212]. Interestingly, μSR measurements revealed evidence for nodal superconductivity in isostructural $ThCoC_2$, where it was suggested that the strong Fermi surface nesting favors an unconventional magnetically mediated pairing mechanism[213]. However, time reversal symmetry was found to be preserved in the superconducting state.

B. Loop-super current state

This proposal[10] is based on a few key observations that the relevant materials (Re_6(Zr, Hf, Ti)[114,123,124], $Re_{0.82}Nb_{0.18}$[115] and La_7(Ir, Rh)$_3$[118,119,124]) have several common features: several symmetry related sites (more than two is necessary) within the unit cell, several Fermi surfaces coming from several orbitals and a single fully gapped conventional BCS type thermodynamic behavior of observables. We consider a uniform onsite singlet pairing and allow for the possibility that the order parameter can potentially have different values (amplitude and phase) at the different symmetry related sites within the unit cell. Then using symmetry it is noted that there is a symmetry allowed ground state which has finite microscopic Josephson currents flowing between the symmetry related sites and is thus termed as a loop-super current (LSC) state. Such a ground state has inherent chirality and thus breaks TRS spontaneously at T_c. An example of such a symmetry allowed order parameter for a system with a $\mathcal{C}_4$ point group and four symmetrically distinct sites has been considered in the Ref. 10. The degeneracy in one of the irreps of $\mathcal{C}_4$ in this case actually comes from TRS in the normal state itself. On symmetry grounds, such a ground state can be stabilized in Re_6(Zr, Hf, Ti)[114,123,124] and $Re_{0.82}Nb_{0.18}$[115] but is not favorable energetically for La_7(Ir, Rh)$_3$[118,119,124]. One of the attractions of the LSC state is that since it only relies on on-site pairing, it does not require an unconvenitonal pairing mechanism. On the other hand, the question of competition with other, more conventional states cannot be addressed within GL theory and is currently unexplored.

C. Symmetry analysis including orbitals – the case of Sr_2RuO_4

In addition to the novel ground states proposed in the previous section, for some materials in particular Sr_2RuO_4 different experiments with high quality samples give apparently conflicting results[214]. It has now become increasingly clear that the common chiral p-wave triplet state[7] with $\boldsymbol{d}$-vector pointing along the c-axis proposed in this material based on the usual symmetry classification discussed earlier cannot systematically account for all/most of the experimental signatures in this material as noted in Section III. Based on this observation, recent studies[208,209,215] have proposed that in this case it is essential to generalize the symmetry classification of the order parameters to include the orbital degrees of freedom as well. This way novel symmetrically allowed possibilities of singlet, triplet with in-plane $\boldsymbol{d}$-vector and mixed parity superconducting ground states[208,209,215] have been proposed which may be able to explain all/most of the features in this material.

D. Bogoliubov Fermi surfaces

It was shown recently[206,207] that for a multiband SC with centrosymmetry and spontaneously broken TRS at T_c, considering the internal electronic degrees of freedom in Cooper pair formation in general leads to only two possible types of quasiparticle excitation gaps: either the system is fully gapped or it has Bogoliubov Fermi surfaces (BFS). These are two dimensional surfaces which are generated, for example, by inflating a point or a line node

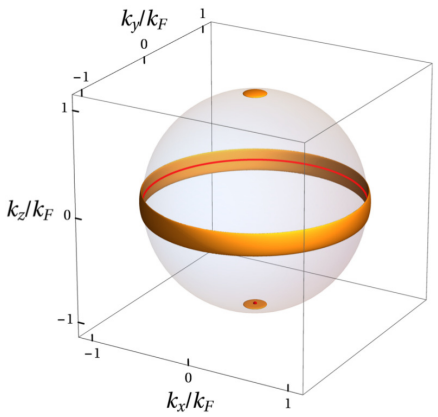

FIG. 10. (Color online) Bogoliubov Fermi surfaces corresponding to the chiral d-wave singlet superconducting state given in Eqn. (29), shown here for the case where only one band has a spherical Fermi surface (semitransparent sphere) for a centrosymmetric multiband SC with generic symmetries and spontaneously breaking TRS at T_c. The point and line nodes (red dots and line, respectively), are "inflated" into spheroidal and toroidal Bogoliubov Fermi surfaces (orange surfaces) protected by a Z_2 topological invariant. Reproduced from Ref. 206. Copyright 2017 by the American Physical Society.

by a pseudo-magnetic field inherent to the TRS breaking nodal superconducting state. An example is shown in the Fig. 10. This pseudo-magnetic field however is proportional to the second order of interband pairing. As a result its strength is quite small. But, the BFSs are protected by a Z_2 topological invariant and hence cannot be removed by symmetry preserving perturbations. A superconducting state possessing BFSs can have characteristic experimental signatures[217] such as a nonzero residual DOS at the Fermi level which can potentially be measured in a single particle tunneling experiment and unconventional thermodynamic signatures at low temperatures. But since the strength of the pseudo-magnetic field which basically distinguishes these type of states from their "trivial" counterparts is generically small, it may turn out to be difficult to distinguish them in practice.

VIII. SUMMARY AND OUTLOOK

In this review we have discussed unconventional SCs which have been recently discovered to break time-reversal symmetry, in addition to gauge symmetry. The picture that emerges from these systems is complex and diverse, but at the same time there are some elements in common and that distinguish them from earlier examples of broken TRS in correlated SCs. First of all, the SCs in question appear, in many ways, conventional: they have nodeless quasiparticle spectra; T_c is insensitive to non-magnetic impurities; and their normal state is often an ordinary Fermi liquid. Secondly, they often have multi-band electronic structures, often with complex unit cells having many symmetry-related atomic sites. These suggest that there are common mechanisms for broken TRS which present themselves in multi-orbital SCs.

The small family formed by $LaNiC_2$ and $LaNiGa_2$ deserves a special mention. While it is usually very hard to pin down what the pairing symmetry is for a given unconventional SC, there has been remarkable progress in the last few years on these two compounds. These systems have very low symmetry, and as a result there are very few possibilities to choose from. The observation of broken TRS at T_c from zero-field μSR is only compatible with equal-spin, nonunitary triplet pairing. This led to the prediction of a sub-dominant magnetization accompanying the superconducting order parameter, which was subsequently confirmed experimentally. The nodeless, two-gap behaviour observed in these systems further points to a common origin of the superconductivity and the excellent agreement of a semi-phenomenological theory based on these ideas with a single adjustable parameter with measurements suggests that these are the first TRS-breaking SCs for which we have a complete and accurate picture of the superconducting state– though understanding the origin of the pairing interaction remains a mystery.

While many SCs with broken TRS show other signs of unconventional pairing, independent confirmation specifically of broken TRS is usually hard to obtain. It has been obtained through the optical Kerr effect in Sr_2RuO_4 and UPt_3 and $PrOs_4Sb_{12}$, as well as through bulk SQUID measurements of magnetization in $LaNiC_2$. Obtaining such evidence for other systems is therefore extremely urgent, as is a better understanding of the way the muon interacts with the crystal and with the superconducting condensate. In this respect we wish to highlight the challenge posed by the very consistent relation between the nuclear moments and muon spin relaxation rate in Re-based SCs[115].

We also note that many of these materials are in the dirty limit. Their resilience in the face of disorder distinguishes them quite clearly from other (particularly nodal) unconventional SCs. An understanding of the effect of disorder on the exotic states described in the last part of this review is a pending issue that will need to be addressed.

To conclude, we note that the macroscopic quantum coherence of SCs makes them inherently useful materials out of which to build qubits[218]– indeed, recently the historic milestone of quantum supremacy has recently been claimed using a superconducting quantum computer [219]. Looking at the future, unconventional SCs offer additional degrees of freedom and therefore potentially could offer routes to novel qubit architectures. The varied phenomenology of the SCs with broken TRS reviewed here suggests that they may be fertile ground to essay such technologies, in particular in the cases where TRS breaking potentially occurs in a triplet pairing state. Realizing

such promise will require not only detailed, quantitative theories of the equilibrium state of such systems, but also a precise understanding of their dynamics. For instance, one could investigate whether the net magnetization of a nonunitary triplet pairing SC like $LaNiC_2$ or $LaNiGa_2$ may show coherent oscillations (in contrast to the magnetization of a ferromagnet, which relaxes quickly). That could make possible qubits based on spin, rather than charge currents. Likewise the chirality of loop supercurrents could potentially be used to encode quantum information as well.

IX. ACKNOWLEDGEMENTS

We acknowledge K. Miyake and F. Steglich for fruitful discussions. This work was supported by the National Key R&D Program of China (Grants No. 2017YFA0303100 and No. 2016YFA0300202), and the National Natural Science Foundation of China (No. 11874320, No. 11974306 and No. U1632275). SKG, JQ and JFA are supported by EPSRC through the project "Unconventional Superconductors: New paradigms for new materials" (grant references EP/P00749X/1 and EP/P007392/1).

* S.Ghosh@kent.ac.uk
† msmidman@zju.edu.cn
‡ hqyuan@zju.edu.cn

[1] P. W. Anderson, More is different, Science **177**, 393 (1972).
[2] M. S. Dresselhaus, G. Dresselhaus, and A. Jorio, *Group theory: application to the physics of condensed matter* (Springer Science & Business Media, 2007).
[3] S. Blundell, *Magnetism in Condensed Matter* (Oxford University Press Oxford, 2001).
[4] A. Ashtekar, J. Olmedo, and P. Singh, Quantum transfiguration of kruskal black holes, Phys. Rev. Lett. **121**, 241301 (2018).
[5] A. Ashtekar, J. Olmedo, and P. Singh, Quantum extension of the kruskal spacetime, Phys. Rev. D **98**, 126003 (2018).
[6] M. Tinkham, *Introduction to superconductivity* (Courier Corporation, 2004).
[7] A. Mackenzie and Y. Maeno, The superconductivity of Sr_2RuO_4 and the physics of spin-triplet pairing, Rev. Mod. Phys. **75**, 657 (2003).
[8] A. Pustogow, Y. Luo, A. Chronister, Y. S. Su, D. A. Sokolov, F. Jerzembeck, A. P. Mackenzie, C. W. Hicks, N. Kikugawa, S. Raghu, E. D. Bauer, and S. E. Brown, Constraints on the superconducting order parameter in Sr_2RuO_4 from oxygen-17 nuclear magnetic resonance, Nature **574**, 72 (2019).
[9] A. de Visser, Superconducting Ferromagnets, in *Encyclopedia of Materials: Science and Technology.-2nd ed.* (Elsevier, 2010).
[10] S. K. Ghosh, J. F. Annett, and J. Quintanilla, Time-reversal symmetry breaking in superconductors through loop super-current order, arXiv e-prints , arXiv:1803.02618 (2018), arXiv:1803.02618 [cond-mat.supr-con].
[11] A. D. Hillier, J. Quintanilla, and R. Cywinski, Evidence for time-reversal symmetry breaking in the noncentrosymmetric superconductor $LaNiC_2$, Phys. Rev. Lett. **102**, 117007 (2009).
[12] J. Quintanilla, A. D. Hillier, J. F. Annett, and R. Cywinski, Relativistic analysis of the pairing symmetry of the noncentrosymmetric superconductor $LaNiC_2$, Phys. Rev. B **82**, 174511 (2010).
[13] A. D. Hillier, J. Quintanilla, B. Mazidian, J. F. Annett, and R. Cywinski, Nonunitary triplet pairing in the centrosymmetric superconductor $LaNiGa_2$, Phys. Rev. Lett. **109**, 097001 (2012).
[14] Z. F. Weng, J. L. Zhang, M. Smidman, T. Shang, J. Quintanilla, J. F. Annett, M. Nicklas, G. M. Pang, L. Jiao, W. B. Jiang, Y. Chen, F. Steglich, and H. Q. Yuan, Two-gap superconductivity in $LaNiGa_2$ with nonunitary triplet pairing and even parity gap symmetry, Phys. Rev. Lett. **117**, 027001 (2016).
[15] S. K. Ghosh, G. Csire, P. Whittlesea, J. F. Annett, M. Gradhand, B. Újfalussy, and J. Quintanilla, Quantitative theory of triplet pairing in the unconventional superconductor $LaNiGa_2$, Phys. Rev. B (R) **101**, 100506 (2020).
[16] T. Holstein, R. E. Norton, and P. Pincus, de Haas-van Alphen effect and the specific heat of an electron gas, Phys. Rev. B **8**, 2649 (1973).
[17] A. Yaouanc and P. D. De Reotier, *Muon spin rotation, relaxation, and resonance: applications to condensed matter*, Vol. 147 (Oxford University Press Oxford, 2011).
[18] S. J. Blundell, Spin-polarized muons in condensed matter physics, Contemp. Phys. **40**, 175 (1999).
[19] J. E. Sonier, J. H. Brewer, and R. F. Kiefl, μsr studies of the vortex state in type-II superconductors, Rev. Mod. Phys. **72**, 769 (2000).
[20] R. Khasanov and Z. Guguchia, Probing the multi gap behavior within '11' and '122' families of iron based superconductors: the muon-spin rotation studies, Supercond. Sci. Technol **28**, 034003 (2015).
[21] J. Xia, Y. Maeno, P. T. Beyersdorf, M. M. Fejer, and A. Kapitulnik, High resolution polar Kerr effect measurements of Sr_2RuO_4: Evidence for broken time-reversal symmetry in the superconducting state, Phys. Rev. Lett. **97**, 167002 (2006).
[22] E. R. Schemm, W. J. Gannon, C. M. Wishne, W. P. Halperin, and A. Kapitulnik, Observation of broken time-reversal symmetry in the heavy-fermion superconductor UPt_3, Science **345**, 190 (2014).

[23] E. R. Schemm, R. E. Baumbach, P. H. Tobash, F. Ronning, E. D. Bauer, and A. Kapitulnik, Evidence for broken time-reversal symmetry in the superconducting phase of URu_2Si_2, Phys. Rev. B **91**, 140506 (2015).

[24] E. R. Schemm, E. M. Levenson-Falk, and A. Kapitulnik, Polar Kerr effect studies of time reversal symmetry breaking states in heavy fermion superconductors, Physica C **535**, 13 (2017).

[25] E. M. Levenson-Falk, E. R. Schemm, Y. Aoki, M. B. Maple, and A. Kapitulnik, Polar Kerr effect from time-reversal symmetry breaking in the heavy-fermion superconductor $PrOs_4Sb_{12}$, Phys. Rev. Lett. **120**, 187004 (2018).

[26] J. Xia, P. T. Beyersdorf, M. M. Fejer, and A. Kapitulnik, Modified Sagnac interferometer for high-sensitivity magneto-optic measurements at cryogenic temperatures, Appl. Phys. Lett. **89**, 062508 (2006).

[27] A. Kapitulnik, J. Xia, E. Schemm, and A. Palevski, Polar Kerr effect as probe for time-reversal symmetry breaking in unconventional superconductors, New J. Phys. **11**, 055060 (2009).

[28] S. Ran, C. Eckberg, Q.-P. Ding, Y. Furukawa, T. Metz, S. R. Saha, I.-L. Liu, M. Zic, H. Kim, J. Paglione, and N. P. Butch, Nearly ferromagnetic spin-triplet superconductivity, Science **365**, 684 (2019).

[29] T. Metz, S. Bae, S. Ran, I.-L. Liu, Y. S. Eo, W. T. Fuhrman, D. F. Agterberg, S. M. Anlage, N. P. Butch, and J. Paglione, Point-node gap structure of the spin-triplet superconductor UTe_2, Phys. Rev. B **100**, 220504 (2019).

[30] S. K. P., D. Singh, P. K. Biswas, G. B. G. Stenning, A. D. Hillier, and R. P. Singh, Investigations of the superconducting ground state of Zr_3Ir: Introducing a new noncentrosymmetric superconductor, Phys. Rev. Materials **3**, 104802 (2019).

[31] T. Shang, S. K. Ghosh, L. J. Chang, C. Baines, M. K. Lee, J. Z. Zhao, J. A. T. Verezhak, D. J. Gawryluk, E. Pomjakushina, M. Shi, M. Medarde, J. Mesot, J. Quintanilla, and T. Shiroka, Time-reversal symmetry breaking in the noncentrosymmetric Zr_3Ir superconductor, Phys. Rev. B (R) **102**, 020503 (2020).

[32] R. H. Heffner, J. L. Smith, J. O. Willis, P. Birrer, C. Baines, F. N. Gygax, B. Hitti, E. Lippelt, H. R. Ott, A. Schenck, E. A. Knetsch, J. A. Mydosh, and D. E. MacLaughlin, New phase diagram for (U,Th)Be_{13}: A muon-spin-resonance and H_{C1} study, Phys. Rev. Lett. **65**, 2816 (1990).

[33] G. M. Luke, Y. Fudamoto, K. M. Kojima, M. I. Larkin, J. Merrin, B. Nachumi, Y. J. Uemura, Y. Maeno, Z. Q. Mao, Y. Mori, H. Nakamura, and M. Sigrist, Time-reversal symmetry-breaking superconductivity in Sr_2RuO_4, Nature **394**, 558 (1998).

[34] A. Sumiyama, D. Kawakatsu, J. Gouchi, A. Yamaguchi, G. Motoyama, Y. Hirose, R. Settai, and Y. Ōnuki, Spontaneous magnetization of non-centrosymmetric superconductor $LaNiC_2$, J. Phys. Soc. Jpn. **84**, 013702 (2015).

[35] H. R. Ott, H. Rudigier, T. M. Rice, K. Ueda, Z. Fisk, and J. L. Smith, p-wave superconductivity in UBe_{13}, Phys. Rev. Lett. **52**, 1915 (1984).

[36] H. R. Ott, H. Rudigier, Z. Fisk, and J. L. Smith, Phase transition in the superconducting state of $U_{1-x}Th_xBe_{13}$ (x=0–0.06), Phys. Rev. B **31**, 1651 (1985).

[37] M. Sigrist and T. M. Rice, Phenomenological theory of the superconductivity phase diagram of $U_{1-x}Th_xBe_{13}$, Phys. Rev. B **39**, 2200 (1989).

[38] G. M. Luke, A. Keren, L. P. Le, W. D. Wu, Y. J. Uemura, D. A. Bonn, L. Taillefer, and J. D. Garrett, Muon spin relaxation in UPt_3, Phys. Rev. Lett. **71**, 1466 (1993).

[39] R. A. Fisher, S. Kim, B. F. Woodfield, N. E. Phillips, L. Taillefer, K. Hasselbach, J. Flouquet, A. L. Giorgi, and J. L. Smith, Specific heat of UPt_3: Evidence for unconventional superconductivity, Phys. Rev. Lett. **62**, 1411 (1989).

[40] R. Joynt and L. Taillefer, The superconducting phases of UPt_3, Rev. Mod. Phys. **74**, 235 (2002).

[41] I. M. Hayes, D. S. Wei, T. Metz, J. Zhang, Y. S. Eo, S. Ran, S. R. Saha, J. Collini, N. P. Butch, D. F. Agterberg, A. Kapitulnik, and P. J., Weyl superconductivity in UTe_2, arXiv preprint arXiv:2002.02539 (2020).

[42] S. Sundar, S. Gheidi, K. Akintola, A. M. Côté, S. R. Dunsiger, S. Ran, N. P. Butch, S. R. Saha, J. Paglione, and J. E. Sonier, Coexistence of ferromagnetic fluctuations and superconductivity in the actinide superconductor UTe_2, Phys. Rev. B **100**, 140502 (2019).

[43] J. A. Sauls, The order parameter for the superconducting phases of UPt_3, Adv. Phys. **43**, 113 (1994).

[44] P. D. de Réotier, A. Huxley, A. Yaouanc, J. Flouquet, P. Bonville, P. Imbert, P. Pari, P. C. M. Gubbens, and A. M. Mulders, Absence of zero field muon spin relaxation induced by superconductivity in the B phase of UPt_3, Phys. Lett. A **205**, 239 (1995).

[45] R. Feyerherm, A. Amato, C. Geibel, F. N. Gygax, P. Hellmann, R. H. Heffner, D. E. MacLaughlin, R. Müller-Reisener, G. J. Nieuwenhuys, A. Schenck, and F. Steglich, Competition between magnetism and superconductivity in $CeCu_2Si_2$, Phys. Rev. B **56**, 699 (1997).

[46] W. Higemoto, A. Koda, R. Kadono, Y. Kawasaki, Y. Haga, D. Aoki, R. Settai, H. Shishido, and Y. Ōnuki, μSR studies on heavy fermion superconductors $CeIrIn_5$ and $CeCoIn_5$, J. Phys. Soc. Jpn. **71**, 1023 (2002).

[47] R. F. Kiefl, J. H. Brewer, I. Affleck, J. F. Carolan, P. Dosanjh, W. N. Hardy, T. Hsu, R. Kadono, J. R. Kempton, S. R. Kreitzman, Q. Li, A. H. O'Reilly, T. M. Riseman, P. Schleger, P. C. E. Stamp, H. Zhou, L. P. Le, G. M. Luke, B. Sternlieb, Y. J. Uemura, H. R. Hart, and K. W. Lay, Search for anomalous internal magnetic fields in high-T_c superconductors as evidence for broken time-reversal symmetry, Phys. Rev. Lett. **64**, 2082 (1990).

[48] H. Saadaoui, Z. Salman, T. Prokscha, A. Suter, H. Huhtinen, P. Paturi, and E. Morenzoni, Absence of spontaneous magnetism associated with a possible time-reversal symmetry breaking state beneath the surface of (110)-oriented $YBa_2Cu_3O_{7-\delta}$ superconducting films, Phys. Rev. B **88**, 180501 (2013).

[49] P. L. Russo, C. R. Wiebe, Y. J. Uemura, A. T. Savici, G. J. MacDougall, J. Rodriguez, G. M. Luke, N. Kaneko, H. Eisaki, M. Greven, O. P. Vajk, S. Ono, Y. Ando, K. Fujita, K. M. Kojima, and S. Uchida, Muon spin relaxation study of superconducting $Bi_2Sr_{2-x}La_xCuO_{6+\delta}$, Phys. Rev. B **75**, 054511 (2007).

[50] Z. L. Mahyari, A. Cannell, C. Gomez, S. Tezok, A. Zelati, E. V. L. de Mello, J.-Q. Yan, D. G. Mandrus, and J. E. Sonier, Zero-field μsr search for a time-reversal-symmetry-breaking mixed pairing state in superconducting $Ba_{1-x}K_xFe_2As_2$, Phys. Rev. B **89**, 020502 (2014).

[51] V. Grinenko, P. Materne, R. Sarkar, H. Luetkens, K. Kihou, C. H. Lee, S. Akhmadaliev, D. V. Efremov, S.-L. Drechsler, and H.-H. Klauss, Superconductiv-

ity with broken time-reversal symmetry in ion-irradiated $\mathbf{Ba_{0.27}K_{0.73}Fe_2As_2}$ single crystals, Phys. Rev. B **95**, 214511 (2017).

[52] V. Grinenko, R. Sarkar, K. Kihou, C. H. Lee, I. Morozov, S. Aswartham, B. Büchner, P. Chekhonin, W. Skrotzki, K. Nenkov, R. Hühne, K. Nielsch, S. L. Drechsler, V. L. Vadimov, M. A. Silaev, P. A. Volkov, I. Eremin, H. Luetkens, and H.-H. Klauss, Superconductivity with broken time-reversal symmetry inside a superconducting s-wave state, Nature Physics 10.1038/s41567-020-0886-9 (2020).

[53] Y. Aoki, A. Tsuchiya, T. Kanayama, S. R. Saha, H. Sugawara, H. Sato, W. Higemoto, A. Koda, K. Ohishi, K. Nishiyama, and R. Kadono, Time-reversal symmetry-breaking superconductivity in heavy-fermion $PrOs_4Sb_{12}$ detected by muon-spin relaxation, Phys. Rev. Lett. **91**, 067003 (2003).

[54] L. Shu, W. Higemoto, Y. Aoki, A. D. Hillier, K. Ohishi, K. Ishida, R. Kadono, A. Koda, O. O. Bernal, D. E. MacLaughlin, Y. Tunashima, Y. Yonezawa, S. Sanada, D. Kikuchi, H. Sato, H. Sugawara, T. U. Ito, and M. B. Maple, Suppression of time-reversal symmetry breaking superconductivity in $Pr(Os_{1-x}Ru_x)_4Sb_{12}$ and $Pr_{1-y}La_yOs_4Sb_{12}$, Phys. Rev. B **83**, 100504 (2011).

[55] A. Maisuradze, W. Schnelle, R. Khasanov, R. Gumeniuk, M. Nicklas, H. Rosner, A. Leithe-Jasper, Y. Grin, A. Amato, and P. Thalmeier, Evidence for time-reversal symmetry breaking in superconducting $PrPt_4Ge_{12}$, Phys. Rev. B **82**, 024524 (2010).

[56] J. Zhang, Z. F. Ding, K. Huang, C. Tan, A. D. Hillier, P. K. Biswas, D. E. MacLaughlin, and L. Shu, Broken time-reversal symmetry in superconducting $Pr_{1-x}La_xPt_4Ge_{12}$, Phys. Rev. B **100**, 024508 (2019).

[57] K. Ishida, H. Mukuda, Y. Kitaoka, K. Asayama, Z. Q. Mao, Y. Mori, and Y. Maeno, Spin-triplet superconductivity in Sr_2RuO_4 identified by ^{17}O Knight shift, Nature **396**, 658 (1998).

[58] J. A. Duffy, S. M. Hayden, Y. Maeno, Z. Mao, J. Kulda, and G. J. McIntyre, Polarized-neutron scattering study of the cooper-pair moment in Sr_2RuO_4, Phys. Rev. Lett. **85**, 5412 (2000).

[59] C. W. Hicks, D. O. Brodsky, E. A. Yelland, A. S. Gibbs, J. A. N. Bruin, M. E. Barber, S. D. Edkins, K. Nishimura, S. Yonezawa, Y. Maeno, and A. P. Mackenzie, Strong increase of T_c of Sr_2RuO_4 under both tensile and compressive strain, Science **344**, 283 (2014).

[60] C. W. Hicks, J. R. Kirtley, T. M. Lippman, N. C. Koshnick, M. E. Huber, Y. Maeno, W. M. Yuhasz, M. B. Maple, and K. A. Moler, Limits on superconductivity-related magnetization in Sr_2RuO_4 and $PrOs_4Sb_{12}$ from scanning SQUID microscopy, Phys. Rev. B **81**, 214501 (2010).

[61] P. J. Curran, S. J. Bending, W. M. Desoky, A. S. Gibbs, S. L. Lee, and A. P. Mackenzie, Search for spontaneous edge currents and vortex imaging in Sr_2RuO_4 mesostructures, Phys. Rev. B **89**, 144504 (2014).

[62] K. I. Wysokiński, Time reversal symmetry breaking superconductors: Sr2RuO4 and beyond, Condensed Matter **4**, 47 (2019).

[63] A. N. Petsch, M. Zhu, M. Enderle, Z. Q. Mao, Y. Maeno, and S. M. Hayden, Reduction of the spin susceptibility in the superconducting state of Sr_2RuO_4 observed by polarized neutron scattering, arXiv preprint arXiv:2002.02856 (2020).

[64] R. Sharma, S. D. Edkins, Z. Wang, A. Kostin, C. Sow, Y. Maeno, A. P. Mackenzie, J. C. S. Davis, and V. Madhavan, Momentum resolved superconducting energy gaps of Sr_2RuO_4 from quasiparticle interference imaging, ArXiv e-prints (2019), arXiv:1912.02798.

[65] S. Kashiwaya, K. Saitoh, H. Kashiwaya, M. Koyanagi, M. Sato, K. Yada, Y. Tanaka, and Y. Maeno, Time-reversal invariant superconductivity of Sr_2RuO_4 revealed by Josephson effects, Phys. Rev. B **100**, 094530 (2019).

[66] V. Grinenko, S. Ghosh, R. Sarkar, J.-C. Orain, A. Nikitin, M. Elender, D. Das, Z. Guguchia, F. Brückner, M. E. Barber, J. Park, N. Kikugawa, D. A. Sokolov, J. S. Bobowski, T. Miyoshi, Y. Maeno, A. P. Mackenzie, H. Luetkens, C. W. Hicks, and H.-H. Klauss, Split superconducting and time-reversal symmetry-breaking transitions, and magnetic order in Sr_2RuO_4 under uniaxial stress, arXiv preprint arXiv:2001.08152 (2020).

[67] S. Ghosh, A. Shekhter, F. Jerzembeck, N. Kikugawa, D. Sokolov, M. Brando, A. P. Mackenzie, C. W. Hicks, and B. J. Ramshaw, Thermodynamic evidence for a two-component superconducting order parameter in Sr_2RuO_4, arXiv preprint arXiv:2002.06130 (2020).

[68] S. Benhabib, C. Lupien, I. Paul, L. Berges, M. Dion, M. Nardone, A. Zitouni, Z. Q. Mao, Y. Maeno, A. Georges, L. Taillefer, and C. Proust, Jump in the c_{66} shear modulus at the superconducting transition of Sr_2RuO_4: Evidence for a two-component order parameter, arXiv preprint arXiv:2002.05916 (2020).

[69] R. Carmi, E. Polturak, G. Koren, and A. Auerbach, Spontaneous macroscopic magnetization at the superconducting transition temperature of $YBa_2Cu_3O_{7-\delta}$, Nature **404**, 853 (2000).

[70] A. Kaminski, S. Rosenkranz, H. M. Fretwell, J. C. Campuzano, Z. Li, H. Raffy, W. G. Cullen, H. You, C. G. Olson, C. M. Varma, and H. Höchst, Spontaneous breaking of time-reversal symmetry in the pseudogap state of a high-T_c superconductor, Nature **416**, 610 (2002).

[71] J. Xia, E. Schemm, G. Deutscher, S. A. Kivelson, D. A. Bonn, W. N. Hardy, R. Liang, W. Siemons, G. Koster, M. M. Fejer, and A. Kapitulnik, Polar Kerr-effect measurements of the high-temperature $YBa_2Cu_3O_{6+x}$ superconductor: Evidence for broken symmetry near the pseudogap temperature, Phys. Rev. Lett. **100**, 127002 (2008).

[72] I. I. Mazin, D. J. Singh, M. D. Johannes, and M. H. Du, Unconventional superconductivity with a sign reversal in the order parameter of $LaFeAsO_{1-x}F_x$, Phys. Rev. Lett. **101**, 057003 (2008).

[73] H. Ding, P. Richard, K. Nakayama, K. Sugawara, T. Arakane, Y. Sekiba, A. Takayama, S. Souma, T. Sato, T. Takahashi, Z. Wang, X. Dai, Z. Fang, G. F. Chen, J. L. Luo, and N. L. Wang, Observation of Fermi-surface–dependent nodeless superconducting gaps in $Ba_{0.6}K_{0.4}Fe_2As_2$, EPL (Europhysics Letters) **83**, 47001 (2008).

[74] K. Nakayama, T. Sato, P. Richard, Y.-M. Xu, Y. Sekiba, S. Souma, G. F. Chen, J. L. Luo, N. L. Wang, H. Ding, and T. Takahashi, Superconducting gap symmetry of $Ba_{0.6}K_{0.4}Fe_2As_2$ studied by angle-resolved photoemission spectroscopy, EPL (Europhysics Letters) **85**, 67002 (2009).

[75] M. Hiraishi, R. Kadono, S. Takeshita, M. Miyazaki, A. Koda, H. Okabe, and J. Akimitsu, Full gap superconductivity in $Ba_{0.6}K_{0.4}Fe_2As_2$ probed by muon spin rotation, J. Phys. Soc. Jpn. **78**, 023710 (2009).

[76] H. Fukazawa, Y. Yamada, K. Kondo, T. Saito, Y. Kohori, K. Kuga, Y. Matsumoto, S. Nakatsuji, H. Kito, P. M. Shirage, K. Kihou, N. Takeshita, C.-H. Lee, A. Iyo, and H. Eisaki, Possible multiple gap superconductivity with line nodes in heavily hole-doped superconductor KFe_2As_2 studied by ^{75}As nuclear quadrupole resonance and specific heat, J. Phys. Soc. Jpn. **78**, 083712 (2009).

[77] J. K. Dong, S. Y. Zhou, T. Y. Guan, H. Zhang, Y. F. Dai, X. Qiu, X. F. Wang, Y. He, X. H. Chen, and S. Y. Li, Quantum criticality and nodal superconductivity in the feas-based superconductor KFe_2As_2, Phys. Rev. Lett. **104**, 087005 (2010).

[78] J.-P. Reid, M. A. Tanatar, A. Juneau-Fecteau, R. T. Gordon, S. R. de Cotret, N. Doiron-Leyraud, T. Saito, H. Fukazawa, Y. Kohori, K. Kihou, C. H. Lee, A. Iyo, H. Eisaki, R. Prozorov, and L. Taillefer, Universal heat conduction in the iron arsenide superconductor KFe_2As_2: Evidence of a d-wave state, Phys. Rev. Lett. **109**, 087001 (2012).

[79] S. Maiti, M. M. Korshunov, T. A. Maier, P. J. Hirschfeld, and A. V. Chubukov, Evolution of the superconducting state of Fe-based compounds with doping, Phys. Rev. Lett. **107**, 147002 (2011).

[80] W.-C. Lee, S.-C. Zhang, and C. Wu, Pairing state with a time-reversal symmetry breaking in FeAs-based superconductors, Phys. Rev. Lett. **102**, 217002 (2009).

[81] K. Okazaki, Y. Ota, Y. Kotani, W. Malaeb, Y. Ishida, T. Shimojima, T. Kiss, S. Watanabe, C.-T. Chen, K. Kihou, C. H. Lee, A. Iyo, H. Eisaki, T. Saito, H. Fukazawa, Y. Kohori, K. Hashimoto, T. Shibauchi, Y. Matsuda, H. Ikeda, H. Miyahara, R. Arita, A. Chainani, and S. Shin, Octet-line node structure of superconducting order parameter in KFe_2As_2, Science **337**, 1314 (2012).

[82] K. Cho, M. Kończykowski, S. Teknowijoyo, M. A. Tanatar, Y. Liu, T. A. Lograsso, W. E. Straszheim, V. Mishra, S. Maiti, P. J. Hirschfeld, and R. Prozorov, Energy gap evolution across the superconductivity dome in single crystals of $(Ba_{1-x}K_x)Fe_2As_2$, Science Advances **2**, 10.1126/sciadv.1600807 (2016).

[83] S. Maiti and A. V. Chubukov, $s + is$ state with broken time-reversal symmetry in fe-based superconductors, Phys. Rev. B **87**, 144511 (2013).

[84] V. L. Vadimov and M. A. Silaev, Polarization of the spontaneous magnetic field and magnetic fluctuations in $s+is$ anisotropic multiband superconductors, Phys. Rev. B **98**, 104504 (2018).

[85] I. Shirotani, T. Uchiumi, K. Ohno, C. Sekine, Y. Nakazawa, K. Kanoda, S. Todo, and T. Yagi, Superconductivity of filled skutterudites $LaRu_4As_{12}$ and $PrRu_4As_{12}$, Phys. Rev. B **56**, 7866 (1997).

[86] N. Takeda and M. Ishikawa, Superconducting and magnetic properties of filled skutterudite compounds $RERu_4Sb_{12}$ (RE = La, Ce, Pr, Nd and Eu), J. Phys. Soc. Jpn. **69**, 868 (2000).

[87] E. D. Bauer, N. A. Frederick, P.-C. Ho, V. S. Zapf, and M. B. Maple, Superconductivity and heavy fermion behavior in $PrOs_4Sb_{12}$, Phys. Rev. B **65**, 100506 (2002).

[88] E. Bauer, A. Grytsiv, X.-Q. Chen, N. Melnychenko-Koblyuk, G. Hilscher, H. Kaldarar, H. Michor, E. Royanian, G. Giester, M. Rotter, R. Podloucky, and P. Rogl, Superconductivity in novel Ge-based skutterudites: Sr, $BaPt_4Ge_{12}$, Phys. Rev. Lett. **99**, 217001 (2007).

[89] R. Gumeniuk, W. Schnelle, H. Rosner, M. Nicklas, A. Leithe-Jasper, and Y. Grin, Superconductivity in the platinum germanides MPt_4Ge_{12} (M = Rare−Earth or alkaline-earth metal) with filled skutterudite structure, Phys. Rev. Lett. **100**, 017002 (2008).

[90] X. Y. Tee, H. G. Luo, T. Xiang, D. Vandervelde, M. B. Salamon, H. Sugawara, H. Sato, C. Panagopoulos, and E. E. M. Chia, Penetration depth study of $LaOs_4Sb_{12}$: Multiband s-wave superconductivity, Phys. Rev. B **86**, 064518 (2012).

[91] E. E. M. Chia, M. B. Salamon, H. Sugawara, and H. Sato, Probing the superconducting gap symmetry of $PrRu_4Sb_{12}$: A comparison with $PrOs_4Sb_{12}$, Phys. Rev. B **69**, 180509 (2004).

[92] H. Pfau, M. Nicklas, U. Stockert, R. Gumeniuk, W. Schnelle, A. Leithe-Jasper, Y. Grin, and F. Steglich, Superconducting gap structure of the skutterudite $LaPt_4Ge_{12}$ probed by specific heat and thermal transport, Phys. Rev. B **94**, 054523 (2016).

[93] M. Shimizu, H. Amanuma, K. Hachitani, H. Fukazawa, Y. Kohori, T. Namiki, C. Sekine, and I. Shirotani, ^{75}As-NQR studies of superconducting filled skutterudites $PrRu_4As_{12}$ and $LaRu_4As_{12}$, J. Phys. Soc. Jpn **76**, 104705 (2007).

[94] T. Cichorek, A. C. Mota, F. Steglich, N. A. Frederick, W. M. Yuhasz, and M. B. Maple, Pronounced enhancement of the lower critical field and critical current deep in the superconducting state of $PrOs_4Sb_{12}$, Phys. Rev. Lett. **94**, 107002 (2005).

[95] L. S. Sharath Chandra, M. K. Chattopadhyay, and S. . Roy, Evidence for two superconducting gaps in the unconventional superconductor $PrPt_4Ge_{12}$, Phil. Mag. **92**, 3866 (2012).

[96] R. W. Hill, S. Li, M. B. Maple, and L. Taillefer, Multiband order parameters for the $PrOs_4Sb_{12}$ and $PrRu_4Sb_{12}$ skutterudite superconductors from thermal conductivity measurements, Phys. Rev. Lett. **101**, 237005 (2008).

[97] G. Seyfarth, J. P. Brison, M.-A. Méasson, J. Flouquet, K. Izawa, Y. Matsuda, H. Sugawara, and H. Sato, Multiband superconductivity in the heavy fermion compound $PrOs_4Sb_{12}$, Phys. Rev. Lett. **95**, 107004 (2005).

[98] G. Seyfarth, J. P. Brison, M.-A. Méasson, D. Braithwaite, G. Lapertot, and J. Flouquet, Superconducting $PrOs_4Sb_{12}$: A thermal conductivity study, Phys. Rev. Lett. **97**, 236403 (2006).

[99] L. Shu, D. E. MacLaughlin, W. P. Beyermann, R. H. Heffner, G. D. Morris, O. O. Bernal, F. D. Callaghan, J. E. Sonier, W. M. Yuhasz, N. A. Frederick, and M. B. Maple, Penetration depth, multiband superconductivity, and absence of muon-induced perturbation in superconducting $PrOs_4Sb_{12}$, Phys. Rev. B **79**, 174511 (2009).

[100] H. Kotegawa, M. Yogi, Y. Imamura, Y. Kawasaki, G.-q. Zheng, Y. Kitaoka, S. Ohsaki, H. Sugawara, Y. Aoki, and H. Sato, Evidence for unconventional strong-coupling superconductivity in $PrOs_4Sb_{12}$: An Sb nuclear quadrupole resonance study, Phys. Rev. Lett. **90**, 027001 (2003).

[101] E. E. M. Chia, M. B. Salamon, H. Sugawara, and H. Sato, Probing the superconducting gap symmetry of $PrOs_4Sb_{12}$: A penetration depth study, Phys. Rev. Lett. **91**, 247003 (2003).

[102] K. Izawa, Y. Nakajima, J. Goryo, Y. Matsuda, S. Osaki, H. Sugawara, H. Sato, P. Thalmeier, and K. Maki, Multiple superconducting phases in new heavy fermion superconductor $PrOs_4Sb_{12}$, Phys. Rev. Lett. **90**, 117001 (2003).

[103] M. Yogi, H. Kotegawa, Y. Imamura, G.-q. Zheng, Y. Kitaoka, H. Sugawara, and H. Sato, Sb-NQR probe for superconducting properties in the Pr-based filled-skutterudite compound $PrRu_4Sb_{12}$, Phys. Rev. B **67**, 180501 (2003).

[104] A. Maisuradze, M. Nicklas, R. Gumeniuk, C. Baines, W. Schnelle, H. Rosner, A. Leithe-Jasper, Y. Grin, and R. Khasanov, Superfluid density and energy gap function of superconducting $PrPt_4Ge_{12}$, Phys. Rev. Lett. **103**, 147002 (2009).

[105] J. L. Zhang, Y. Chen, L. Jiao, R. Gumeniuk, M. Nicklas, Y. H. Chen, L. Yang, B. H. Fu, W. Schnelle, H. Rosner, A. Leithe-Jasper, Y. Grin, F. Steglich, and H. Q. Yuan, Multiband superconductivity in $PrPt_4Ge_{12}$ single crystals, Phys. Rev. B **87**, 064502 (2013).

[106] J. L. Zhang, G. M. Pang, L. Jiao, M. Nicklas, Y. Chen, Z. F. Weng, M. Smidman, W. Schnelle, A. Leithe-Jasper, A. Maisuradze, C. Baines, R. Khasanov, A. Amato, F. Steglich, R. Gumeniuk, and H. Q. Yuan, Weak interband-coupling superconductivity in the filled skutterudite $LaPt_4Ge_{12}$, Phys. Rev. B **92**, 220503 (2015).

[107] F. Kanetake, H. Mukuda, Y. Kitaoka, K.-i. Magishi, H. Sugawara, K. M. Itoh, and E. E. aller, Superconducting characteristics of filled skutterudites $LaPt_4Ge_{12}$ and $PrPt_4Ge_{12}$: ^{73}Ge-NQR/NMR studies, J. Phys. Soc. Jpn **79**, 063702 (2010).

[108] Y. Nakamura, H. Okazaki, R. Yoshida, T. Wakita, H. Takeya, K. Hirata, M. Hirai, Y. Muraoka, and T. Yokoya, Comparative photoemission studies on the superconducting gap of the filled skutterudite superconductors $LaPt_4Ge_{12}$ and $PrPt_4Ge_{12}$, Phys. Rev. B **86**, 014521 (2012).

[109] N. L. Zeng and W. H. Lee, Superconductivity in the ni-based ternary compound $LaNiGa_2$, Phys. Rev. B **66**, 092503 (2002).

[110] W. Lee, H. Zeng, Y. Yao, and Y. Chen, Superconductivity in the Ni based ternary carbide $LaNiC_2$, Physica C: Superconductivity **266**, 138 (1996).

[111] V. K. Pecharsky, L. L. Miller, and K. A. Gschneidner, Low-temperature behavior of two ternary lanthanide nickel carbides: Superconducting $LaNiC_2$ and magnetic $CeNiC_2$, Phys. Rev. B **58**, 497 (1998).

[112] J. Chen, L. Jiao, J. L. Zhang, Y. Chen, L. Yang, M. Nicklas, F. Steglich, and H. Q. Yuan, Evidence for two-gap superconductivity in the non-centrosymmetric compound $LaNiC_2$, New J. Phys. **15**, 053005 (2013).

[113] Y. Iwamoto, Y. Iwasaki, K. Ueda, and T. Kohara, Microscopic measurements in ^{139}La-NQR of the ternary carbide superconductor $LaNiC_2$, Phys. Lett. A **250**, 439 (1998).

[114] R. P. Singh, A. D. Hillier, B. Mazidian, J. Quintanilla, J. F. Annett, D. M. Paul, G. Balakrishnan, and M. R. Lees, Detection of time-reversal symmetry breaking in the noncentrosymmetric superconductor Re_6Zr using muon-spin spectroscopy, Phys. Rev. Lett. **112**, 107002 (2014).

[115] T. Shang, M. Smidman, S. K. Ghosh, C. Baines, L. J. Chang, D. J. Gawryluk, J. A. T. Barker, R. P. Singh, D. M. Paul, G. Balakrishnan, E. Pomjakushina, M. Shi, M. Medarde, A. D. Hillier, H. Q. Yuan, J. Quintanilla, J. Mesot, and T. Shiroka, Time-reversal symmetry breaking in Re-based superconductors, Phys. Rev. Lett. **121**, 257002 (2018).

[116] G. M. Pang, Z. Y. Nie, A. Wang, D. Singh, W. Xie, W. B. Jiang, Y. Chen, R. P. Singh, M. Smidman, and H. Q. Yuan, Fully gapped superconductivity in single crystals of noncentrosymmetric Re_6Zr with broken time-reversal symmetry, Phys. Rev. B **97**, 224506 (2018).

[117] T. Shang, M. Smidman, A. Wang, L.-J. Chang, C. Baines, M. K. Lee, Z. Y. Nie, G. M. Pang, W. Xie, W. B. Jiang, M. Shi, M. Medarde, T. Shiroka, and H. Q. Yuan, Simultaneous nodal superconductivity and time-reversal symmetry breaking in the noncentrosymmetric superconductor CaPtAs, Phys. Rev. Lett. **124**, 207001 (2020).

[118] J. A. T. Barker, D. Singh, A. Thamizhavel, A. D. Hillier, M. R. Lees, G. Balakrishnan, D. M. Paul, and R. P. Singh, Unconventional superconductivity in La_7Ir_3 revealed by muon spin relaxation: Introducing a new family of noncentrosymmetric superconductor that breaks time-reversal symmetry, Phys. Rev. Lett. **115**, 267001 (2015).

[119] B. Li, C. Q. Xu, W. Zhou, W. H. Jiao, R. Sankar, F. M. Zhang, H. H. Hou, X. F. Jiang, B. Qian, B. Chen, A. F. Bangura, and X. Xu, Evidence of s-wave superconductivity in the noncentrosymmetric La_7Ir_3, Scientific Reports **8**, 651 (2018).

[120] D. Singh, M. S. Scheurer, A. D. Hillier, and R. P. Singh, Time-reversal-symmetry breaking and unconventional pairing in the noncentrosymmetric superconductor La_7Rh_3 probed by μSR, ArXiv e-prints (2018), arXiv:1802.01533.

[121] B. T. Matthias, V. B. Compton, and E. Corenzwit, Some new superconducting compounds, J. Phys. Chem. Solids **19**, 130 (1961).

[122] R. D. Blaugher and J. K. Hulm, Superconductivity in the σ and α-Mn structures, J. Phys. Chem. Solids **19**, 134 (1961).

[123] D. Singh, J. A. T. Barker, A. Thamizhavel, D. McK. Paul, A. D. Hillier, and R. P. Singh, Time-reversal symmetry breaking in noncentrosymmetric superconductor Re_6Hf: further evidence for unconventional behaviour in the alpha-Mn family of materials, ArXiv e-prints (2017), arXiv:1710.08598.

[124] D. Singh, S. K. P., J. A. T. Barker, D. M. Paul, A. D. Hillier, and R. P. Singh, Time-reversal symmetry breaking in the noncentrosymmetric superconductor Re_6Ti, Phys. Rev. B **97**, 100505 (2018).

[125] T. Shang, G. M. Pang, C. Baines, W. B. Jiang, W. Xie, A. Wang, M. Medarde, E. Pomjakushina, M. Shi, J. Mesot, H. Q. Yuan, and T. Shiroka, Nodeless superconductivity and time-reversal symmetry breaking in the noncentrosymmetric superconductor $Re_{24}Ti_5$, Phys. Rev. B **97**, 020502 (2018).

[126] C. Cirillo, R. Fittipaldi, M. Smidman, G. Carapella, C. Attanasio, A. Vecchione, R. P. Singh, M. R. Lees, G. Balakrishnan, and M. Cuoco, Evidence of double-gap superconductivity in noncentrosymmetric $Nb_{0.18}Re_{0.82}$ single crystals, Phys. Rev. B **91**, 134508 (2015).

[127] P. Parab, D. Singh, S. Haram, R. P. Singh, and S. Bose, Point contact Andreev reflection studies of a noncentrosymmetric superconductor Re_6Zr, Sci. Rep. **9**, 2498 (2019).

[128] C. S. Lue, H. F. Liu, C. N. Kuo, P. S. Shih, J. Y. Lin, Y. K. Kuo, M. W. Chu, T. L. Hung, and Y. Y. Chen, Investigation of normal and superconducting states in noncentrosymmetric $Re_{24}Ti_5$, Supercond. Sci. Technol. **26**, 055011 (2013).

[129] J. Chen, L. Jiao, J. L. Zhang, Y. Chen, L. Yang, M. Nicklas, F. Steglich, and H. Q. Yuan, BCS-like superconductivity in the noncentrosymmetric compounds Nb_xRe_{1-x} ($0.13 \leq x \leq 0.38$), Phys. Rev. B **88**, 144510 (2013).

[130] B. Chen, Y. Guo, H. Wang, Q. Su, Q. Mao, J. Du, Y. Zhou, J. Yang, and M. Fang, Superconductivity in the noncentrosymmetric compound Re_6Hf, Phys. Rev. B **94**, 024518 (2016).

[131] M. A. Khan, A. B. Karki, T. Samanta, D. Browne, S. Stadler, I. Vekhter, A. Pandey, P. W. Adams, D. P. Young, S. Teknowijoyo, K. Cho, R. Prozorov, and D. E. Graf, Complex superconductivity in the noncentrosymmetric compound Re_6Zr, Phys. Rev. B **94**, 144515 (2016).

[132] K. Matano, R. Yatagai, S. Maeda, and G.-q. Zheng, Full-gap superconductivity in noncentrosymmetric Re_6Zr, $Re_{27}Zr_5$, and $Re_{24}Zr_5$, Phys. Rev. B **94**, 214513 (2016).

[133] D. A. Mayoh, J. A. T. Barker, R. P. Singh, G. Balakrishnan, D. M. Paul, and M. R. Lees, Superconducting and normal-state properties of the noncentrosymmetric superconductor Re_6Zr, Phys. Rev. B **96**, 064521 (2017).

[134] Q. Huang, T. Le, L. Che, L. Yin, J. Li, J. Yang, M. Fang, and X. Lu, A single full gap in noncentrosymmetric superconductor Re_6Hf by point-contact spectroscopy, Mater. Res. Express **6**, 016001 (2018).

[135] A. A. Aczel, T. J. Williams, T. Goko, J. P. Carlo, W. Yu, Y. J. Uemura, T. Klimczuk, J. D. Thompson, R. J. Cava, and G. M. Luke, Muon spin rotation/relaxation measurements of the noncentrosymmetric superconductor $Mg_{10}Ir_{19}B_{16}$, Phys. Rev. B **82**, 024520 (2010).

[136] D. Singh, J. A. T. Barker, A. Thamizhavel, A. D. Hillier, D. M. Paul, and R. P. Singh, Superconducting properties and μSR study of the noncentrosymmetric superconductor $Nb_{0.5}Os_{0.5}$, J. Phys.: Condens. Matter **30**, 075601 (2018).

[137] P. K. Biswas, A. D. Hillier, M. R. Lees, and D. M. Paul, Comparative study of the centrosymmetric and noncentrosymmetric superconducting phases of Re_3W using muon spin spectroscopy and heat capacity measurements, Phys. Rev. B **85**, 134505 (2012).

[138] Y. Nishikubo, K. Kudo, and M. Nohara, Superconductivity in the honeycomb-lattice pnictide SrPtAs, J. Phys. Soc. Jpn. **80**, 055002 (2011).

[139] M. H. Fischer, F. Loder, and M. Sigrist, Superconductivity and local noncentrosymmetricity in crystal lattices, Phys. Rev. B **84**, 184533 (2011).

[140] J. Goryo, M. H. Fischer, and M. Sigrist, Possible pairing symmetries in SrPtAs with a local lack of inversion center, Phys. Rev. B **86**, 100507 (2012).

[141] W.-S. Wang, Y. Yang, and Q.-H. Wang, Triplet f-wave pairing in SrPtAs, Phys. Rev. B **90**, 094514 (2014).

[142] M. H. Fischer, T. Neupert, C. Platt, A. P. Schnyder, W. Hanke, J. Goryo, R. Thomale, and M. Sigrist, Chiral d-wave superconductivity in SrPtAs, Phys. Rev. B **89**, 020509 (2014).

[143] K. Matano, K. Arima, S. Maeda, Y. Nishikubo, K. Kudo, M. Nohara, and G.-q. Zheng, Spin-singlet superconductivity with a full gap in locally noncentrosymmetric SrPtAs, Phys. Rev. B **89**, 140504 (2014).

[144] F. Brückner, R. Sarkar, M. Günther, H. Kühne, H. Luetkens, T. Neupert, A. P. Reyes, P. L. Kuhns, P. K. Biswas, T. Stürzer, D. Johrendt, and H.-H. Klauss, Multigap superconductivity in locally noncentrosymmetric SrPtAs: An ^{75}As nuclear quadrupole resonance investigation, Phys. Rev. B **90**, 220503 (2014).

[145] J. F. Landaeta, S. V. Taylor, I. Bonalde, C. Rojas, Y. Nishikubo, K. Kudo, and M. Nohara, High-resolution magnetic penetration depth and inhomogeneities in locally noncentrosymmetric SrPtAs, Phys. Rev. B **93**, 064504 (2016).

[146] W. Xie, P. Zhang, B. Shen, W. Jiang, G. Pang, T. Shang, C. Cao, M. Smidman, and H. Yuan, CaPtAs: A new noncentrosymmetric superconductor, Science China Physics, Mechanics & Astronomy **63**, 237412 (2020).

[147] W. H. Lee, F. A. Yang, C. R. Shih, and H. D. Yang, Crystal structure and superconductivity in the Ni-based ternary compound LaNiSi, Phys. Rev. B **50**, 6523 (1994).

[148] J. Evers, G. Oehlinger, A. Weiss, and C. Probst, Superconductivity of LaPtSi and LaPtGe, Solid State Commun. **50**, 61 (1984).

[149] F. Kneidinger, H. Michor, A. Sidorenko, E. Bauer, I. Zeiringer, P. Rogl, C. Blaas-Schenner, D. Reith, and R. Podloucky, Synthesis, characterization, electronic structure, and phonon properties of the noncentrosymmetric superconductor LaPtSi, Phys. Rev. B **88**, 104508 (2013).

[150] Y. Qi, J. Guo, H. Lei, Z. Xiao, T. Kamiya, and H. Hosono, Superconductivity in noncentrosymmetric ternary equiatomic pnictides LaMP (M = Ir and Rh; P = P and As), Phys. Rev. B **89**, 024517 (2014).

[151] K. Domieracki and D. Kaczorowski, Superconductivity in a non-centrosymmetric compound ThCoSi, J. Alloys Compd. **688**, 206 (2016).

[152] K. P. Sajilesh, D. Singh, P. K. Biswas, A. D. Hillier, and R. P. Singh, Superconducting properties of the noncentrosymmetric superconductor LaPtGe, Phys. Rev. B **98**, 214505 (2018).

[153] A. Ptok, K. Domieracki, K. J. Kapcia, J. Łażewski, P. T. Jochym, M. Sternik, P. Piekarz, and D. Kaczorowski, Electronic and lattice properties of noncentrosymmetric superconductors ThTSi (T = Co, Ir, Ni, and Pt), Phys. Rev. B **100**, 165130 (2019).

[154] P. Zhang, H. Q. Yuan, and C. Cao, Electron-phonon coupling and nontrivial band topology in noncentrosymmetric superconductors LaNiSi, LaPtSi, and LaPtGe, Phys. Rev. B **101**, 245145 (2020).

[155] G. Wenski and A. Mewis, Ternäre varianten des AlB_2-typs. darstellung und struktur von Ca(Eu)PtX (X = P, As, Sb), $CaPt_xP_{2-x}$, EuPtxP(As_{2-x} und $CaPt_xAs_{0,9}$, Z. Anorg. Allg. Chem. **543**, 49 (1986).

[156] J. Remeika, G. Espinosa, A. Cooper, H. Barz, J. Rowell, D. McWhan, J. Vandenberg, D. Moncton, Z. Fisk, L. Woolf, H. Hamaker, M. Maple, G. Shirane, and W. Thomlinson, A new family of ternary intermetallic superconducting/magnetic stannides, Solid State Commun. **34**, 923 (1980).

[157] A. Bhattacharyya, D. T. Adroja, J. Quintanilla, A. D. Hillier, N. Kase, A. M. Strydom, and J. Akimitsu, Broken time-reversal symmetry probed by muon spin relaxation in the caged type superconductor $Lu_5Rh_6Sn_{18}$, Phys. Rev. B **91**, 060503 (2015).

[158] A. Bhattacharyya, D. T. Adroja, N. Kase, A. D. Hillier, J. Akimitsu, and A. Strydom, Unconventional superconductivity in $\mathbf{Y_5Rh_6Sn_{18}}$ probed by muon spin relaxation, Scientific Reports **5**, 12926 (2015).

[159] A. Bhattacharyya, D. T. Adroja, N. Kase, A. D. Hillier, A. M. Strydom, and J. Akimitsu, Unconventional superconductivity in the cage-type compound $\mathbf{Sc_5Rh_6Sn_{18}}$, Phys. Rev. B **98**, 024511 (2018).

[160] Z. Zhang, Y. Xu, C. N. Kuo, X. C. Hong, M. X. Wang, P. L. Cai, J. K. Dong, C. S. Lue, and S. Y. Li, Nodeless superconducting gap in the caged-type superconduc-

tors $Y_5Rh_6Sn_{18}$ and $Lu_5Rh_6Sn_{18}$, Supercond. Sci. Technol. **28**, 105008 (2015).
[161] N. Kase, S. Kittaka, T. Sakakibara, and J. Akimitsu, Superconducting gap structure of the cage compound $Sc_5Rh_6Sn_{18}$, J. Phys. Soc. Jpn. **81**, SB016 (2012).
[162] N. Kase, S. Kittaka, T. Sakakibara, and J. Akimitsu, Anisotropic superconductivity of the caged compound $Y_5Rh_6Sn_{18}$ with unusual normal-state electrical resistivity, JPS Conf. Proc. **3**, 015042 (2014).
[163] N. Kase, K. Inoue, H. Hayamizu, and J. Akimitsu, Highly anisotropic gap function in a nonmagnetic superconductor $Y_5Rh_6Sn_{18}$, J. Phys. Soc. Jpn. **80**, SA112 (2011).
[164] G. Volovik and L. Gor'kov, Superconducting classes in heavy-fermion systems, in *30 Years Of The Landau Institute - Selected Papers* (World Scientific, 1996) pp. 258–269.
[165] J. F. Annett, Symmetry of the order parameter for high-temperature superconductivity, Advances in Physics **39**, 83 (1990).
[166] M. Sigrist and K. Ueda, Phenomenological theory of unconventional superconductivity, Rev. Mod. Phys. **63**, 239 (1991).
[167] J.-C. Toledano and P. Toledano, *The Landau theory of phase transitions: application to structural, incommensurate, magnetic and liquid crystal systems*, Vol. 3 (World Scientific Publishing Company, 1987).
[168] P. W. Anderson, *Basic notions of condensed matter physics* (CRC Press, 2018).
[169] E. I. Blount, Symmetry properties of triplet superconductors, Phys. Rev. B **32**, 2935 (1985).
[170] Y. Yanase, Nonsymmorphic Weyl superconductivity in UPt_3 based on E_{2u} representation, Phys. Rev. B **94**, 174502 (2016).
[171] S. Sumita, T. Nomoto, and Y. Yanase, Multipole superconductivity in nonsymmorphic Sr_2IrO_4, Phys. Rev. Lett. **119**, 027001 (2017).
[172] T. Micklitz and M. R. Norman, Symmetry-enforced line nodes in unconventional superconductors, Phys. Rev. Lett. **118**, 207001 (2017).
[173] S. Sumita and Y. Yanase, Unconventional superconducting gap structure protected by space group symmetry, Phys. Rev. B **97**, 134512 (2018).
[174] M. Smidman, M. B. Salamon, H. Q. Yuan, and D. F. Agterberg, Superconductivity and spin-orbit coupling in non-centrosymmetric materials: a review, Rep. Prog. Phys. **80**, 036501 (2017).
[175] P. Coleman, *Introduction to many-body physics* (Cambridge University Press, 2015).
[176] C. Kallin and J. Berlinsky, Chiral superconductors, Rep. Prog. Phys. **79**, 054502 (2016).
[177] D. J. Singh, Electronic structure and fermiology of superconducting $LaNiGa_2$, Phys. Rev. B **86**, 174507 (2012).
[178] M. Sato and Y. Ando, Topological superconductors: a review, Rep. Prog. Phys. **80**, 076501 (2017).
[179] Y. Tanaka, M. Sato, and N. Nagaosa, Symmetry and topology in superconductors–odd-frequency pairing and edge states–, J. Phys. Soc. Jpn. **81**, 011013 (2011).
[180] A. P. Schnyder, S. Ryu, A. Furusaki, and A. W. W. Ludwig, Classification of topological insulators and superconductors in three spatial dimensions, Phys. Rev. B **78**, 195125 (2008).
[181] A. P. Schnyder and P. M. R. Brydon, Topological surface states in nodal superconductors, J. Phys.: Condens. Matter **27**, 243201 (2015).
[182] B. Béri, Topologically stable gapless phases of time-reversal-invariant superconductors, Phys. Rev. B **81**, 134515 (2010).
[183] A. P. Schnyder, P. M. R. Brydon, and C. Timm, Types of topological surface states in nodal noncentrosymmetric superconductors, Phys. Rev. B **85**, 024522 (2012).
[184] B. Mazidian, J. Quintanilla, A. Hillier, and J. Annett, Anomalous thermodynamic power laws near topological transitions in nodal superconductors, Phys. Rev. B **88**, 10.1103/PhysRevB.88.224504 (2013).
[185] R. M. Fernandes and J. Schmalian, Scaling of nascent nodes in extended-s-wave superconductors, Phys. Rev. B **84**, 012505 (2011).
[186] C. Beenakker, Search for Majorana fermions in superconductors, Annual Review of Condensed Matter Physics **4**, 113 (2013).
[187] P. Goswami and A. H. Nevidomskyy, Topological Weyl superconductor to diffusive thermal Hall metal crossover in the B phase of UPt_3, Phys. Rev. B **92**, 214504 (2015).
[188] L. Jiao, S. Howard, S. Ran, Z. Wang, J. O. Rodriguez, M. Sigrist, Z. Wang, N. P. Butch, and V. Madhavan, Chiral superconductivity in heavy-fermion metal UTe_2, Nature **579**, 523 (2020).
[189] D. Shoenberg, *Low Temperature Physics LT9* (Springer US, 1965) pp. 665–676.
[190] S. Hufner, *Photoelectron Spectroscopy : Principles and Applications* (Springer Berlin Heidelberg, Berlin, Heidelberg, 2003).
[191] K. Capelle, A birdś-eye view of density-functional theory, Brazilian Journal of Physics **36**, 1318 (2006).
[192] T. Oguchi, Electronic band structure of the superconductor Sr_2RuO_4, Phys. Rev. B **51**, 1385 (1995).
[193] D. J. Singh, Relationship of Sr_2RuO_4 to the superconducting layered cuprates, Phys. Rev. B **52**, 1358 (1995).
[194] I. Hase and T. Yanagisawa, Electronic structure of $LaNiGa_2$, J. Phys. Soc. Jpn. **81**, 103704 (2012).
[195] H. M. Tütüncü and G. P. Srivastava, Origin of superconductivity in layered centrosymmetric $LaNiGa_2$, Appl. Phys. Lett. **104**, 022603 (2014).
[196] K. Miyake and A. Tsuruta, Theory for Intrinsic Magnetic Field in Chiral Superconductor Measured by μSR: Case of Sr_2RuO_4, arXiv e-prints , arXiv:1709.09388 (2017), arXiv:1709.09388 [cond-mat.supr-con].
[197] J. Robbins, J. F. Annett, and M. Gradhand, Modern Theory for the Orbital Moment in a Superconductor, arXiv e-prints , arXiv:1802.10533 (2018), arXiv:1802.10533 [cond-mat.supr-con].
[198] K. Miyake, *Private communication* (2018).
[199] F. R. Foronda, F. Lang, J. S. Möller, T. Lancaster, A. T. Boothroyd, F. L. Pratt, S. R. Giblin, D. Prabhakaran, and S. J. Blundell, Anisotropic local modification of crystal field levels in Pr-based pyrochlores: A muon-induced effect modeled using density functional theory, Phys. Rev. Lett. **114**, 017602 (2015).
[200] I. J. Onuorah, P. Bonfà, R. De Renzi, L. Monacelli, F. Mauri, M. Calandra, and I. Errea, Quantum effects in muon spin spectroscopy within the stochastic self-consistent harmonic approximation, Phys. Rev. Materials **3**, 073804 (2019).
[201] M. Tinkham, *Introduction to Superconductivity* (McGraw-Hill Inc., 1996).
[202] D. J. Scalapino, A common thread: The pairing interaction for unconventional superconductors, Rev. Mod. Phys. **84**, 1383 (2012).

[203] T. Nomoto, K. Hattori, and H. Ikeda, Classification of "multipole" superconductivity in multiorbital systems and its implications, Phys. Rev. B **94**, 174513 (2016).

[204] P. M. R. Brydon, L. Wang, M. Weinert, and D. F. Agterberg, Pairing of $j = 3/2$ fermions in half-Heusler superconductors, Phys. Rev. Lett. **116**, 177001 (2016).

[205] E. M. Nica, R. Yu, and Q. Si, Orbital-selective pairing and superconductivity in iron selenides, npj Quantum Materials **2**, 24 (2017).

[206] D. F. Agterberg, P. M. R. Brydon, and C. Timm, Bogoliubov Fermi surfaces in superconductors with broken time-reversal symmetry, Phys. Rev. Lett. **118**, 127001 (2017).

[207] P. M. R. Brydon, D. F. Agterberg, H. Menke, and C. Timm, Bogoliubov Fermi surfaces: General theory, magnetic order, and topology, Phys. Rev. B **98**, 224509 (2018).

[208] W. Huang, Y. Zhou, and H. Yao, Exotic Cooper pairing in multiorbital models of Sr_2RuO_4, Phys. Rev. B **100**, 134506 (2019).

[209] A. Ramires and M. Sigrist, Superconducting order parameter of Sr_2RuO_4: A microscopic perspective, Phys. Rev. B **100**, 104501 (2019).

[210] G. Csire, B. Újfalussy, and J. F. Annett, Nonunitary triplet pairing in the noncentrosymmetric superconductor $LaNiC_2$, The European Physical Journal B **91**, 217 (2018).

[211] K. Miyake, Theory of pairing assisted spin polarization in spin-triplet equal spin pairing: Origin of extra magnetization in Sr_2RuO_4 in superconducting state, J. Phys. Soc. Jpn. **83**, 053701 (2014).

[212] J. F. Landaeta, D. Subero, P. Machado, F. Honda, and I. Bonalde, Unconventional superconductivity and an ambient-pressure magnetic quantum critical point in single-crystal $LaNiC_2$, Phys. Rev. B **96**, 174515 (2017).

[213] A. Bhattacharyya, D. T. Adroja, K. Panda, S. Saha, T. Das, A. J. S. Machado, O. V. Cigarroa, T. W. Grant, Z. Fisk, A. D. Hillier, and P. Manfrinetti, Evidence of a nodal line in the superconducting gap symmetry of noncentrosymmetric $ThCoC_2$, Phys. Rev. Lett. **122**, 147001 (2019).

[214] A. P. Mackenzie, T. Scaffidi, C. W. Hicks, and Y. Maeno, Even odder after twenty-three years: the superconducting order parameter puzzle of Sr_2RuO_4, npj Quantum Materials **2**, 40 (2017).

[215] S.-O. Kaba and D. Sénéchal, Group-theoretical classification of superconducting states of strontium ruthenate, Phys. Rev. B **100**, 214507 (2019).

[216] C. Setty, S. Bhattacharyya, Y. Cao, A. Kreisel, and P. Hirschfeld, Topological ultranodal pair states in iron-based superconductors, Nature communications **11**, 1 (2020).

[217] C. J. Lapp, G. Börner, and C. Timm, Experimental consequences of Bogoliubov Fermi surfaces, arXiv e-prints , arXiv:1909.10370 (2019), arXiv:1909.10370 [cond-mat.supr-con].

[218] M. H. Devoret, A. Wallraff, and J. M. Martinis, Superconducting qubits: A short review (2004), arXiv:cond-mat/0411174 [cond-mat.mes-hall].

[219] F. Arute, K. Arya, R. Babbush, D. Bacon, J. C. Bardin, R. Barends, R. Biswas, S. Boixo, F. G. Brandao, D. A. Buell, *et al.*, Quantum supremacy using a programmable superconducting processor, Nature **574**, 505 (2019).